

# Provisioning Short-Term Traffic Fluctuations in Elastic Optical Networks

Zhizhen Zhong<sup>1b</sup>, *Student Member, IEEE*, Nan Hua, *Member, IEEE*, Massimo Tornatore, *Senior Member, IEEE*,  
Jialong Li<sup>1b</sup>, Yanhe Li, Xiaoping Zheng<sup>1b</sup>, and Biswanath Mukherjee<sup>1b</sup>, *Fellow, IEEE*

**Abstract**—Transient traffic spikes are becoming a crucial challenge for network operators from both user-experience and network-maintenance perspectives. Different from long-term traffic growth, the bursty nature of short-term traffic fluctuations makes it difficult to be provisioned effectively. Luckily, next-generation elastic optical networks (EONs) provide an economical way to deal with such short-term traffic fluctuations. In this paper, we go beyond conventional network reconfiguration approaches by proposing the novel lightpath-splitting scheme in EONs. In lightpath splitting, we introduce the concept of SplitPoints to describe how lightpath splitting is performed. Lightpaths traversing multiple nodes in the optical layer can be split into shorter ones by SplitPoints to serve more traffic demands by raising signal modulation levels of lightpaths accordingly. We formulate the problem into a mathematical optimization model and linearize it into an integer linear program (ILP). We solve the optimization model on a small network instance and design scalable heuristic algorithms based on greedy and simulated annealing approaches. Numerical results show the tradeoff between throughput gain and negative impacts like traffic interruptions. Especially, by selecting SplitPoints wisely, operators can achieve almost twice as much throughput as conventional schemes without lightpath splitting.

**Index Terms**—Network reconfiguration, traffic fluctuations, elastic optical networks, lightpath splitting, network optimization.

## I. INTRODUCTION

IS RUNNING the network with much excess capacity the only effective way to accommodate sudden and short-term traffic fluctuations? Surely, a larger capacity means less congestion, and more requests can be served, leading to improved user experience and higher income. Unfortunately, adding more network capacity will increase both Capital Expenditures (CapEx) and Operational Expenditures (OpEx). Conventional network management schemes are based on the assumption that spikes during traffic fluctuations are not so severe, which was indeed true in the past. Hence, a common way to accommodate traffic fluctuations consisted in dimensioning network

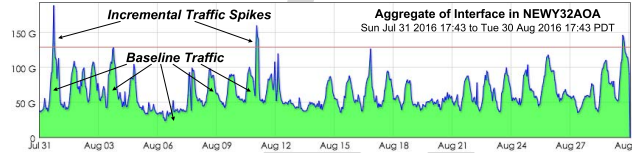


Fig. 1. Aggregated traffic fluctuations of New York in Internet2 network (accessed 30 Aug 2016 PDT, via <http://snapp2.blcd.gnrc.iu.edu/i2net/>).

capacity based on traffic spikes [1], [2], and turning some network equipment on/off following traffic fluctuations [3]–[6].

Traffic is now becoming more dynamic and bursty than ever before, and this observation motivates operators to revisit the problem of how to effectively accommodate traffic fluctuations. Today, traffic fluctuations with extremely sharp spikes may require bandwidth many times beyond baseline traffic amount, or even several times beyond normal maximum traffic. Two examples illustrate this trend. The first is a recent game, Pokémon GO, which generated traffic 50 times beyond expectations [7], showing how unexpectedly new traffic spikes can occur in the network. Also, specific nation- or world-wide mega events, like Double Eleven in China, Black Friday in the U.S. [8], [9], finals of FIFA World Cup, and Olympic Games [10], induce severe traffic spikes. These spikes are generated by millions of users standing out of their daily habits, and usually last for only few hours, or days. Fig. 1 shows an example on how incremental traffic spikes overload the network (50% more than baseline peaks, 200% more than baseline valleys) in a low frequency (twice a month).

Therefore, operators must address a complex tradeoff between service quality at traffic spikes and network cost: *on one hand, providing high performance even in case of occasional sharp spikes requires much larger capacity (over-equipped for most of time, and leading to higher CapEx and OpEx); on the other hand, more conservative capacity dimensioning does not allow to serve traffic spikes effectively (service outages in spike hour may negatively affect subscribers' loyalty)*. Conventional strategies based on turning off idle equipment in a over-provisioned network cannot solve this problem completely, because they can only reduce electricity costs (a part of OpEx), while other parts of OpEx, such as human-resource cost, and CapEx will not be saved. Also, frequent on-off operations driven by daily fluctuations might deteriorate equipment lifetime, leading to high repair cost (OpEx) or need for premature investment on new infrastructures (CapEx) [11]–[13]. Thus, new methods are needed to handle such short-term traffic fluctuations. And this is what we aim to address throughout this study.

Manuscript received March 6, 2018; revised December 27, 2018; accepted May 28, 2019; approved by IEEE/ACM TRANSACTIONS ON NETWORKING Editor S. Subramaniam. This work was supported in part by the NSFC under Grant 61871448 and Grant 61621064, in part by the National Science Foundation under Grant 1716945, and in part by the Networks Lab., UC Davis. (Corresponding author: Xiaoping Zheng.)

Z. Zhong, N. Hua, J. Li, Y. Li, and X. Zheng are with the Beijing National Research Center for Information Science and Technology, Department of Electronic Engineering, Tsinghua University, Beijing 100084, China (e-mail: xpzheng@mail.tsinghua.edu.cn).

M. Tornatore is with the Department of Electronics, Information and Bioengineering, Politecnico di Milano, 20133 Milan, Italy, and also with the Networks Lab., University of California at Davis, Davis, CA 95616 USA.

B. Mukherjee is with the Networks Laboratory, University of California at Davis, Davis, CA 95616 USA.

Digital Object Identifier 10.1109/TNET.2019.2925631

In this work, we present a comprehensive study on provisioning short-term traffic fluctuations under a novel network reconfiguration scheme with lightpath splitting. We summarize our contributions as follows: 1) to the best of our knowledge, this is the first work on provisioning short-term traffic fluctuations in Elastic Optical Networks (EONs) via optical-layer reconfigurations; 2) a novel network reconfiguration scheme with lightpath splitting is devised; 3) we formulate the problem using a mathematical model and acquire its results to guide the design of scalable algorithms; and 4) both greedy and simulated annealing algorithms are proposed to quickly solve the problem. Illustrative results show that we can achieve significant throughput improvement by affecting a fraction of traffic due to reconfiguration under incremental traffic spikes.

The remainder of the study is organized as follows: Section II discusses the role of short-term reconfiguration, and reviews prior works. Section III introduces the lightpath-splitting scheme. Section IV mathematically formulates the problem of lightpath splitting, and obtains its optimization results. Section V devises scalable heuristic algorithms for large network instances. Section VI presents illustrative numerical evaluations by simulation. Section VII concludes this study.

## II. SHORT-TERM RECONFIGURATIONS FOR NETWORK MAINTENANCE AND MANAGEMENT

### A. Role of Short-Term Reconfigurations

We divide short-term traffic fluctuations into two parts: baseline traffic and incremental traffic spikes, as depicted in Fig. 1. Baseline traffic refers to the average daily traffic, while incremental traffic spikes are transient load increases.

Generally, network capacity is sufficient for baseline traffic, and lightpaths are provisioned in a relatively static way (weeks or months without change). If a traffic spike arrives, the network monitor in charge of detecting traffic anomaly [14] will trigger short-term network re-planning and reconfiguration (inner cycle in Fig. 2) based on current network planning result (see the arrow directed from network planning to short-term network re-planning). When short-term spikes leave, those split lightpaths will gradually recover to original longer lightpaths. The details on the recovery process are out of the scope of this paper, and we only discuss spikes provisioning.

Note that short-term reconfiguration is intended as an emergency plan for operators to avoid short-term resource crunch. For longer-term traffic growth, usual periodic network capacity upgrade (outer cycle in Fig. 2) that scales networks out by adding new equipments is important and necessary [15], [16].

### B. Related Work

Many conventional investigations on short-term reconfigurations focused on the energy efficiency gain in a over-provisioned network. Reference [3] presented a strategy to save energy consumption when traffic varies. Reference [4] employed lightpath bypass and router-card sleep modes to minimize energy consumption under daily traffic fluctuation. Reference [5] compared various traffic-aware strategies for energy efficiency. Reference [17] proposed a power-aware traffic management protocol to reduce overheads. Other studies

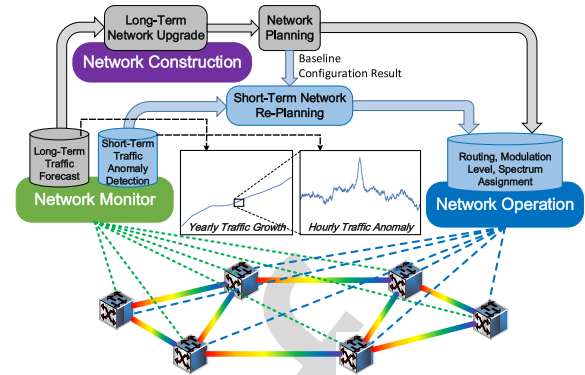


Fig. 2. Short-term reconfigurations in network maintenance and management.

consider the tradeoff between energy efficiency and device lifetime [11]–[13].

Regarding short-term reconfigurations to avoid network congestion, [2] proposed a technique that leveraged a small amount of link capacity to achieve high resource utilization without congestion. Reference [18] studied both short-term traffic variation and long-term traffic growth, and concluded that network re-optimization without optical path re-routing and wavelength defragmentation does not lead to significant performance improvement. This work inspires us to serve traffic fluctuations by optical-layer reconfigurations [19]–[22].

The idea of splitting optical-layer long lightpaths into shorter ones was discussed in [23] for Wavelength-Division-Multiplexed (WDM) networks. Lightpath splitting as a way of network reconfiguration was studied in WDM ring networks with a simple heuristic algorithm [24]. Reference [25] showed that short lightpaths can achieve higher resource utilization and lower blocking probability. In EONs, shorter lightpaths can support higher-order modulations, which in turn increase network capacity [26]. This fact inspires us to devise a solution to exploit the elasticity of the optical layer to accommodate incremental traffic spikes [27], [28]. Experiments also supports quick modulation format reconfiguration [29]–[31].

Different from the above methods that reconfigure network hardware, degraded service provisioning acts as the admission control for bandwidth reconfiguration. The main point for degraded service provisioning lies in the idea that a degraded level of service can be provided (instead of no service at all) when the network becomes congested [32]–[36]. On the joint reconfiguration of both traffic bandwidth and network infrastructures, Reference [37] explored multi-layer degraded service provisioning in EONs. Note that our method benefits from all these previous studies, which inspired us to conceive the idea of lightpath splitting [23]–[28], [32]–[37], as well as to support the feasibility of our approach [29]–[31]. In short, the core contribution of this study with respect to the existing body of literature is the introduction and comprehensive evaluation of lightpath-splitting concept as an amendment of network reconfiguration in EONs to cope with resource crunch during traffic spikes.

## III. LIGHTPATH SPLITTING SCHEME

### A. Principle and Definitions

We consider a network topology in a unidirectional graph:  $G(\mathbf{N}, \mathbf{E})$ , where  $\mathbf{N}$  and  $\mathbf{E}$  denote the set of nodes and fiber

178 links, respectively. Lightpath  $l$  runs through nodes  $N_O(l)$  and  
 179 links  $E_O(l)$  on optical layer,  $N_O(l) \subseteq N$ ,  $E_O(l) \subseteq E$ .  
 180  $S(l)$ ,  $W(l)$ ,  $L(l)$  represent the modulation level (in bits  
 181 per symbol), number of adopted spectrum slots, and length,  
 182 respectively, of lightpath  $l$ .  $F$  is the total number of spec-  
 183 trum slots of a fiber. The transparent reach of modulation  
 184 level  $S(l)$  is  $T[S(l)]$ .

185 **Definition 1 (SplitPoint):** A **SplitPoint** on lightpath  $l$  is  
 186 defined as a tuple  $V_i = [v, l]$ ,  $v \in N_O(l)$ , so that  $l$  is  
 187 split into two segments,  $l_1$ ,  $l_2$ , by  $V_i$ . In this case, we have  
 188  $N_O(l_1) \subsetneq N_O(l)$ ,  $N_O(l_2) \subsetneq N_O(l)$ ,  $N_O(l_1) \cap N_O(l_2) = \{v\}$ ,  
 189  $N_O(l_1) \cup N_O(l_2) = N_O(l)$ , and  $E_O(l_1) \subsetneq E_O(l)$ ,  $E_O(l_2) \subsetneq$   
 190  $E_O(l)$ ,  $E_O(l_1) \cap E_O(l_2) = \emptyset$ ,  $E_O(l_1) \cup E_O(l_2) = E_O(l)$ .

191 **Definition 2 (SplitLightpath & PostSplitLightpath):** If  
 192 lightpath  $l$  is split into  $l_1$  and  $l_2$  by a SplitPoint  $V_i = [v, l]$ ,  $l$   
 193 is a **SplitLightpath**, and  $l_1$  and  $l_2$  are **PostSplitLightpaths**.

194 **Definition 3 (Lightpath Splitting):** Lightpath splitting is  
 195 performed when there are SplitPoints on SplitLightpaths.  
 196 During lightpath splitting, the optical-layer route of the  
 197 SplitLightpath is unchanged, while its adopted spectrum slots  
 198 can be returned. After lightpath splitting, the modulation  
 199 level and data rate of PostSplitLightpaths are guaranteed  
 200 to not decrease.  $S(l)W(l) \leq S(l_1)W(l_1)$  and  $S(l)W(l) \leq$   
 201  $S(l_2)W(l_2)$ .

202 We define two policies for spectrum reallocation of Post-  
 203 SplitLightpaths: the first aims at maximizing electrical-layer  
 204 capacity, named ‘‘MaxE’’, which only raises modulation levels  
 205 of corresponding lightpaths, without shrinking the number of  
 206 adopted spectrum slots. The other one aims at maximizing  
 207 post-split optical-layer capacity, called ‘‘MaxO’’, which raises  
 208 modulation levels while shrinking the number of adopted spec-  
 209 trum slots. During PostSplitLightpaths spectrum allocation, all  
 210 available slots are equally likely to be utilized as long as they  
 211 meet the spectrum continuity and contiguity constraints.

212 **Theorem 1:** For a SplitLightpath  $l$  and its PostSplitLight-  
 213 paths  $l_1$  and  $l_2$ , we have  $\text{Max}\{S(l_1), S(l_2)\} > S(l)$  and  
 214  $\text{Min}\{S(l_1), S(l_2)\} \geq S(l)$ , under half-distance law<sup>1</sup> of  
 215 optical signal transparent reach [26], [38], [39].

216 **Proof:** Based on optical signal transparent reach, we have  
 217  $T[S(l) + 1] < L(l) \leq T[S(l)]$ . Half-distance law ensures  
 218  $T[S(l)] = 2T[S(l) + 1]$ , so  $T[S(l) + 1] < L(l) \leq 2T[S(l) + 1]$ .  
 219 Based on Definitions 1-3,  $L(l) = L(l_1) + L(l_2)$ .

220 If  $L(l_1) > T(S(l) + 1)$ ,  $S(l_1) = S(l)$ . Then,  $L(l_2) < L(l) -$   
 221  $T[S(l) + 1] \leq T[S(l) + 1]$ ,  $S(l_2) \geq S(l) + 1 > S(l)$ . If  $L(l_1) \leq$   
 222  $T[S(l) + 1]$ ,  $S(l_1) \geq S(l) + 1 > S(l)$ . Then,  $L(l_2) = L(l) -$   
 223  $L(l_1) < L(l)$ ,  $S(l_2) \geq S(l)$ . Theorem 1 proved.  $\square$

224 We use a simple example to illustrate how lightpath splitting  
 225 works. As shown in Fig. 3, SplitLightpath A-C originally  
 226 traverses Fibers A-B and B-C with four slots under BPSK.  
 227 If Node B is set to be a SplitPoint, then A-C is split into  
 228 PostSplitLightpath A-B under 16QAM, and PostSplitLightpath  
 229 B-C under QPSK (MaxE does not shrink the spectrum, while  
 230 MaxO does, and both policies may retune the used spectrum  
 231 slots). During this process, optical-layer route is not changed.

<sup>1</sup>Though many experiments have skewed this law by demonstrating  
 higher-order modulation in a longer reach, the universal principle that  
 higher-order modulation signal propagates shorter reach is true. Here,  
 half-distance law acts as a well-known and generic mathematical relationship  
 between transmission reach and modulation level only used to perform  
 theoretical investigations.

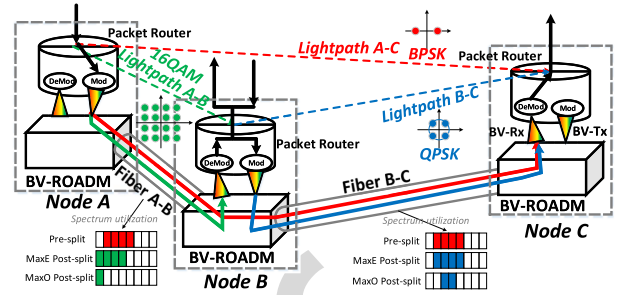


Fig. 3. Illustration of lightpath splitting.

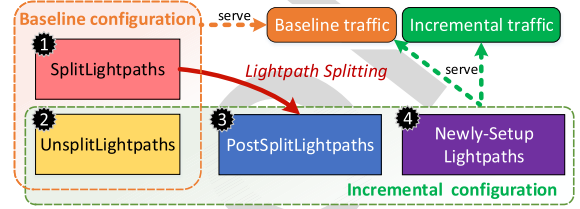


Fig. 4. Conceptual relationships among different kinds of lightpaths.

## B. Relationships of Lightpaths

232 We explain the conceptual relationships among different  
 233 lightpaths in the process of lightpath splitting in Fig. 4.  
 234 Most of the time, operators run their network in baseline  
 235 configuration. When traffic spike arrives, lightpath splitting  
 236 is triggered. A fraction of baseline lightpaths are selected  
 237 to become SplitLightpaths, and they are then split to be PostSplit-  
 238 Lightpaths, while the remainder of baseline lightpaths, named  
 239 UnsplitLightpaths, operate as before. Some lightpath splitting  
 240 operations, like MaxO, can release occupied spectrum slots,  
 241 which enables new lightpaths, i.e., Newly-Setup Lightpaths,  
 242 to be established. The combination of UnsplitLightpaths, Post-  
 243 SplitLightpaths, and Newly-Setup Lightpaths makes up new  
 244 network configuration under traffic spikes.

## C. Capacity Improvement

245 We define function  $\mathcal{F}(l) = S(l)W(l) + S_{max}[F - W(l)]$ ,  
 246 as the capacity<sup>2</sup> of the fiber supporting lightpath  $l$ .

247 **Theorem 2:** Lightpath splitting can increase the total  
 248 capacity of fiber links, which means:  $\text{Max}\{\mathcal{F}(l_1), \mathcal{F}(l_2)\} >$   
 249  $\mathcal{F}(l)$  and  $\text{Min}\{\mathcal{F}(l_1), \mathcal{F}(l_2)\} \geq \mathcal{F}(l)$ .

250 **Proof:** We build our proof on Theorem 1. For MaxO,  
 251 we have:

252 If  $L(l_1) > T(S(l) + 1)$ , we have  $S(l_1) = S(l)$  and  $S(l_2) >$   
 253  $S(l)$ . As  $S(l_1) = S(l)$ , so,  $W(l_1) = W(l)$  and  $\mathcal{F}(l_1) = \mathcal{F}(l)$ .  
 254 As  $S(l_2) > S(l)$ ,  $\frac{W(l)S(l)}{S(l_2)} \leq W(l_2)$ , and  $\mathcal{F}(l_2) = S_{max}F +$   
 255  $W(l_2)[S(l_2) - S_{max}]$ . We replace  $W(l_2)$  and  $S(l_2)$ , and we  
 256 have  $\mathcal{F}(l_2) > S_{max}F + W(l)S(l) - W(l)S_{max} = \mathcal{F}(l)$ .

257 If  $L(l_1) \leq T[S(l) + 1]$ , we have  $S(l_1) > S(l)$  and  $S(l_2) \geq$   
 258  $S(l)$ . Besides,  $W(l_1) \geq \frac{W(l)S(l)}{S(l_1)}$ ,  $W(l_2) \geq \frac{W(l)S(l)}{S(l_2)}$ . We put  
 259 the above four inequalities into the expansions of  $\mathcal{F}(l_1)$  and  
 260  $\mathcal{F}(l_2)$ , then, we have  $\mathcal{F}(l_1) > \mathcal{F}(l)$  and  $\mathcal{F}(l_2) \geq \mathcal{F}(l)$ .

261 For MaxE,  $W(l) = W(l_1) = W(l_2)$ . Theorem 1 can be  
 262 extended to prove Theorem 2.  $\square$

<sup>2</sup>The total capacity of a physical link, i.e., fiber, can be evaluated by  
 the theoretical maximum amount of data that it can support [40]. Here,  
 we consider this capacity to consist of two parts: utilized spectrum for  
 lightpaths, and non-utilized spectrum. For non-utilized spectrum, we treat it  
 as a potential resource and use the highest modulation level available.

265 Note that network capacity is a static concept, which is  
 266 summed up by capacities of links, while network throughput  
 267 is a dynamic concept from user perspectives, jointly decided  
 268 by network capacity, network resource allocation schemes,  
 269 and offered traffic requests. In real networks where traffic  
 270 bandwidth granularities are much smaller than link capacity,  
 271 network capacity becomes the dominant factor for network  
 272 throughput. Therefore, the capacity improvement by lightpath  
 273 splitting can increase network throughput.

#### 274 D. Prerequisites and Applicabilities

275 As a network reconfiguration scheme, the effectiveness of  
 276 lightpath splitting partly relies on baseline network configura-  
 277 tions. To apply lightpath splitting, there are two prerequisites  
 278 on lightpaths and transceivers.

279 *Assumption 1: To perform lightpath splitting, each network  
 280 node should be equipped with enough transceivers.*

281 As we discussed, each added SplitPoint needs a pair of  
 282 transceivers inside that node. In fact, operators usually equip  
 283 extra transceivers at all nodes for backup or protection pur-  
 284 poses, and the number of transceivers is not a constraint.

285 *Assumption 2: To perform lightpath splitting, lightpaths in  
 286 baseline configuration should have the potential to be split.*

287 Here, “the potential to be split” means that a baseline light-  
 288 path  $l$  should be multi-hop in physical layer ( $|\mathbf{N}_O(l)| > 2$ ).  
 289 On modulation levels, if  $S(l)$  is already in the highest mod-  
 290 ulation level and cannot be raised, the effect of modulation  
 291 level increase will not be revealed, and problem then degener-  
 292 ates into existing ones that simply splitting long lightpaths  
 293 into shorter ones for better resource flexibility [22]–[25].  
 294 In practical backbone networks, there will always be some  
 295 lightpaths that traverse multiple physical nodes with thousands  
 296 of kilometers long, and cannot use the highest modulation.

#### 297 E. Negative Impacts

298 The negative impacts of lightpath splitting are from two  
 299 perspectives: in-operation impacts and post-operation impacts.

300 During lightpath splitting, the main negative impact is the  
 301 disruption of existing traffic. Specifically, traffic interruptions  
 302 are caused by tearing down SplitLightpaths and setting up  
 303 PostSplitLightpaths. The most critical barrier during lightpath  
 304 addition and removal is the optical power instability caused by  
 305 wavelength-dependent power excursions of the erbium-doped  
 306 fiber amplifiers (EDFA) which are used for signal amplifica-  
 307 tion in optical networks [41]. Detailed discussions of EDFA  
 308 power fluctuations can be found in [42]–[44]. There are  
 309 several existing techniques to mitigate the power excursions  
 310 and reduce the power adjustment delay [45]–[49]. With these  
 311 methods, the execution of lightpath splitting, which removes  
 312 SplitLightpaths and adds PostSplitLightpaths, can be done  
 313 within several seconds [44].

314 Note also that service interruption can be avoided by  
 315 performing lightpath splitting in advance with proper schedul-  
 316 ing algorithms [50]. Such beforehand operations are feasible  
 317 because the traffic spikes are typically caused by pre-scheduled  
 318 mega-events, which give operators enough time to perform  
 319 lightpath splitting before traffic spikes arrive. Another positive  
 320 aspect is that the baseline network is not fully-occupied, and

usually has certain amount of spare network capacities to per-  
 form hitless capacity configuration by migrating the original  
 traffic from SplitLightpaths to a backup path until lightpath  
 splitting is complete [31] using dependency graphs [51] in  
 a consistent manner. In these ways, the service interruption  
 during lightpath splitting can be alleviated or even eliminated.

After lightpath splitting, the main negative impacts are  
 degradation of end-to-end service latency,<sup>3</sup> and increase of  
 energy consumption, deriving from the fact that traffic requests  
 have to traverse shorter lightpaths (hence more transceivers)  
 on average. It is worth reminding that the number of increased  
 transceivers is equal to twice the number of SplitPoints.

## IV. FORMULATIONS OF LIGHTPATH SPLITTING

Lightpath splitting, as a short-term reconfiguration, is per-  
 formed in a provisioned network that is facing traffic spikes.  
 The baseline lightpaths are set as the input.

### A. The Mathematical Optimization Model

Here, we formulate a mathematical model to serve incre-  
 mental traffic spikes on baseline network configurations  
 (already provisioned). As stated before, the routes of base-  
 line traffic (on both electrical and optical layers) cannot be  
 changed, while it is only the modulation level along with  
 spectrum allocation on optical layer that can be reconfigured.

#### General Parameters:

- $\mathbf{G}(\mathbf{N}, \mathbf{E})$ ,  $T(a)$ ,  $F$ : as defined in Section III.A.
- $\mathbf{A}$ : set of modulation levels  $a$  (in bits per symbol).
- $D(m, n)$ : distance of fiber link  $(m, n)$ .
- $C$ : spectrum slot size (in Hz).
- $M$ : a positive maximum number.
- $\mathbf{R}$ : traffic set composed of  $r = \{s_r, d_r, b_r\}$ , which denotes a request’s source, destination, and bandwidth, respectively.
- $\mu$ : scale parameter controlling the amount of incremental traffic spikes. So, the bandwidth of request  $r$  is  $\mu \cdot b_r$ .
- $\eta_1, \eta_2$ : scaling parameters for the objectives,  $\eta_1 \gg \eta_2$ .

#### Parameters for Baseline Lightpath Configurations:

- $\mathbf{L}$ : set of baseline lightpaths<sup>4</sup>  $l$ .
- $\mathbf{E}_O(l)$ ,  $\mathbf{N}_O(l)$ ,  $S(l)$ ,  $W(l)$ : as defined in Section III.A.
- $H(l)$ : physical-layer hops of baseline lightpath  $l$ .
- $B(l)$ : occupied capacity by baseline traffic on baseline lightpath  $l$ , ensuring the route of baseline traffic is unchanged.

**Binary Variables for Lightpath Splitting:**  $\forall (i, j) \in \mathbf{L}$ ,  
 if  $(i, j)$  is an UnsplitLightpath, all variables below equal 0.  
 But, its modulation level might be increased if necessary.

- $\pi_{(x,y)}^{(i,j)}$ : equals 1 if SplitLightpath  $(i, j)$  is split into PostSplitLightpath  $(x, y)$ .
- $\xi_{(m,n),f}^{(i,j),(x,y)}$ : equals 1 if PostSplitLightpath  $(x, y)$  of SplitLightpath  $(i, j)$  uses fiber  $(m, n)$  on slot  $f$ .

<sup>3</sup>In optical networks, service latency mainly consists of propagation latency (0.005 ms/km) on optical layer, and nodal processing latency in packet routers on electrical layer for packet queuing, traffic grooming, signal multiplexing/demultiplexing at the end of lightpaths. Under the condition of optical-layer route unchanged, the number of traversed lightpaths (hops on electrical layer) is the decisive variable for request latency degradation.

<sup>4</sup>Note that a lightpath  $l$  can also be expressed as  $(i, j)$ , where  $i$  and  $j$  denote source and destination, respectively, of the baseline lightpath.

- 368 •  $\varphi_{(x,y),f}^{(i,j)}$ : equals 1 if PostSplitLightpath  $(x, y)$  of SplitLight-  
 369 path  $(i, j)$  employs slot  $f$ .  
 370 •  $\omega_{(x,y),a}^{(i,j)}$ : equals 1 if PostSplitLightpath  $(x, y)$  of SplitLight-  
 371 path  $(i, j)$  uses modulation level  $a$ .

### 372 Binary Variables for Newly-Setup Lightpaths $(\tilde{i}, \tilde{j})$

- 373 •  $\alpha_{(\tilde{i}, \tilde{j})}^r$ : equals 1 if request  $r$  uses lightpath  $(\tilde{i}, \tilde{j})$  as an  
 374 intermediate electrical-layer link.  
 375 •  $\lambda_{(m,n),f}^{(\tilde{i}, \tilde{j})}$ : equals 1 if lightpath  $(\tilde{i}, \tilde{j})$  uses fiber link  $(m, n)$   
 376 on slot  $f$ .  
 377 •  $\sigma_{(m,n)}^{(\tilde{i}, \tilde{j})}$ : equals 1 if lightpath  $(\tilde{i}, \tilde{j})$  uses fiber link  $(m, n)$ .  
 378 •  $\chi_f^{(\tilde{i}, \tilde{j})}$ : equals 1 if lightpath  $(\tilde{i}, \tilde{j})$  uses slot  $f$ .  
 379 •  $\theta_a^{(\tilde{i}, \tilde{j})}$ : equals 1 if lightpath  $(\tilde{i}, \tilde{j})$  adopts modulation level  $a$ .

380 **Variables for Incremental Traffic Accommodation:** Here,  
 381 if a request's bandwidth cannot be fully accessed, it is allowed  
 382 to serve a fraction of the bandwidth.<sup>5</sup> So, we introduce  $\rho_{\tilde{r}}$  as  
 383 a bandwidth degradation indicator.

- 384 •  $\rho_r$ : integer, actual access bandwidth of request  $r$  under  
 385 resource crunch,  $0 \leq \rho_r \leq b_r$ .  
 386 •  $\varepsilon_r$ : binary, equals 1 if request  $r$  is accessed.

387 **Optimize:** During traffic spikes, lightpath splitting is used  
 388 by the operator to maximize the network throughput as a  
 389 primary goal. As the introduction of SplitPoints poses negative  
 390 impacts on existing traffic, the operator should try to avoid  
 391 unnecessary SplitPoints to mitigate these impacts. There-  
 392 fore, we maximize incremental network throughput first, and  
 393 then minimize total number of SplitPoints second, as shown  
 394 below.

$$395 \quad \text{Maximize: } \eta_1 \cdot \sum_{r \in \mathbf{R}} \rho_r \cdot \varepsilon_r - \eta_2 \cdot \sum_{l \in \mathbf{L}, x, y \in \mathbf{N}} \pi_{(x,y)}^l. \quad (1)$$

### 396 Constraints:

#### 397 1) Optical-Layer Constraints for Lightpath Splitting:

$$398 \quad \sum_{y \in \mathbf{N}_O(i,j)} \pi_{(x,y)}^{(i,j)} - \sum_{y \in \mathbf{N}_O(i,j)} \pi_{(y,x)}^{(i,j)} = \begin{cases} 1, & x = i \\ -1, & x = j \\ 0, & x \neq i, j, \end{cases} \\ 399 \quad \forall (i, j) \in \mathbf{L}, x \in \mathbf{N}_O(i, j). \quad (2)$$

400 Eq. (2) is the lightpath splitting constraint deciding whether  
 401 lightpath  $(i, j)$  is a SplitLightpath, and how to split it.

$$402 \quad \pi_{(x,y)}^l = 0, \quad \forall l \in \mathbf{L}, x, y \in \mathbf{C}_{\mathbf{N}} \mathbf{N}_O(i, j). \quad (3)$$

$$403 \quad \sum_{f \in [1, W]} \varphi_{(x,y),f}^l = 0, \quad \forall l \in \mathbf{L}, x, y \in \mathbf{C}_{\mathbf{N}} \mathbf{N}_O(i, j). \quad (4)$$

$$404 \quad \sum_{a \in \mathbf{A}} \omega_{(x,y),a}^l = 0, \quad \forall l \in \mathbf{L}, x, y \in \mathbf{C}_{\mathbf{N}} \mathbf{N}_O(i, j). \quad (5)$$

$$405 \quad \sum_{f \in [1, W]} \sum_{(m,n) \in \mathbf{E}} \xi_{(m,n),f}^{l,(x,y)} = 0, \quad \forall l \in \mathbf{L}, x, y \in \mathbf{C}_{\mathbf{N}} \mathbf{N}_O(i, j). \\ 406 \quad (6)$$

$$407 \quad \xi_{(m,n),f}^{l,(x,y)} = 0, \quad \forall f \in [1, F], x, y \in \mathbf{N}, l \in \mathbf{L}, (m, n) \in \mathbf{C}_{\mathbf{E}} \mathbf{E}_O(l). \\ 408 \quad (7)$$

$$409 \quad \sum_{(m,n) \in \mathbf{E}_O(l)} \xi_{(m,n),f}^{l,(x,y)} - \sum_{(n,m) \in \mathbf{E}_O(l)} \xi_{(n,m),f}^{l,(x,y)}$$

<sup>5</sup>This electrical-layer bandwidth degradation [32]–[36] is set to fully exploit network capacity to overcome the drawback that served bandwidth of  $r$  is either 0 or  $b_r$ , due to discrete nature of ILP ( $\varepsilon_r$  is binary).

$$= \begin{cases} \varphi_{(x,y),f}^l, & m = x \\ -\varphi_{(x,y),f}^l, & m = y \\ 0, & m \neq x, y, \end{cases} \quad \forall f \in [1, F], x, y \in \mathbf{N}, l \in \mathbf{L}. \quad (8) \quad 411$$

$$1 \leq \sum_{x, y \in \mathbf{N}} \pi_{(x,y)}^l \leq H(l), \quad \forall l \in \mathbf{L}. \quad (9) \quad 412$$

On PostSplitLightpaths routing, Eqs. (3)–(8) ensure that a  
 SplitLightpath is split within its routed nodes set, which means  
 that the optical-layer route is unchanged. Eq. (9) ensures the  
 number of PostSplitLightpaths should be no larger than the  
 number of original lightpath hops of the SplitLightpath.

$$\pi_{(x,y)}^l \leq \sum_{f \in [1, W]} \varphi_{(x,y),f}^l \leq M \cdot \pi_{(x,y)}^l, \quad \forall x, y \in \mathbf{N}, l \in \mathbf{L}. \quad (10) \quad 418 \\ -M \cdot (\varphi_{(x,y),f}^l - \varphi_{(x,y),f+1}^l - 1) \geq \sum_{f' \in [f+2, W]} \varphi_{(x,y),f'}^l, \\ \forall f \in [1, F-1], x, y \in \mathbf{N}, l \in \mathbf{L}. \quad (11) \quad 420$$

On PostSplitLightpaths spectrum allocation, Eq. (10) trig-  
 gers PostSplitLightpaths slot allocation if  $l$  is a SplitLightpath.  
 Eq. (11) is spectrum-consecutive constraint.

$$\sum_{f \in [1, F]} \varphi_{(x,y),f}^l \cdot \sum_{a \in \mathbf{A}} a \cdot \omega_{(x,y),a}^l \geq W(l) \cdot S(l) \cdot \pi_{(x,y)}^l, \\ \forall l \in \mathbf{L}, x, y \in \mathbf{N}. \quad (12) \quad 425$$

$$\sum_{a \in \mathbf{A}} a \cdot \omega_{(x,y),a}^l \geq S(l) \cdot \pi_{(x,y)}^l, \quad \forall l \in \mathbf{L}, x, y \in \mathbf{N}. \quad (13) \quad 426$$

$$\sum_{f \in [1, F]} \varphi_{(x,y),f}^l \leq W(l), \quad \forall l \in \mathbf{L}, x, y \in \mathbf{N}. \quad (14) \quad 427$$

$$\sum_{a \in \mathbf{A}} \omega_{(x,y),a}^l \leq 1, \quad \forall l \in \mathbf{L}, x, y \in \mathbf{N}. \quad (15) \quad 428$$

$$\pi_{(x,y)}^l \leq \sum_{a \in \mathbf{A}} \omega_{(x,y),a}^l \leq M \cdot \pi_{(x,y)}^l, \quad \forall x, y \in \mathbf{N}, l \in \mathbf{L}. \quad (16) \quad 429$$

$$\sum_{(m,n) \in \mathbf{E}} \xi_{(m,n),f}^{l,(x,y)} \cdot D(m, n) \leq T(a) - M \cdot (\omega_{(x,y),a}^l - 1), \\ \forall l \in \mathbf{L}, x, y \in \mathbf{N}, a \in \mathbf{A}, f \in [1, F]. \quad (17) \quad 431$$

$$\sum_{a \in \mathbf{A}} \omega_{(x,y),a}^l \leq \sum_{f \in [1, F]} \varphi_{(x,y),f}^l \leq M \cdot \sum_{a \in \mathbf{A}} \omega_{(x,y),a}^l, \\ \forall l \in \mathbf{L}, x, y \in \mathbf{N}. \quad (18) \quad 433$$

On PostSplitLightpaths modulation level determination,  
 Eqs. (12)–(14) ensure that PostSplitLightpaths have no larger  
 spectrum usage, and no smaller data rate and modulation level  
 than original ones. Eq. (15) ensures PostSplitLightpaths use  
 only one modulation format. Eq. (16) reveals the relationship  
 between modulation level allocation and lightpath splitting.  
 Eq. (17) is PostSplitLightpath maximum-transmission-reach  
 constraint. Eq. (18) describes the relationship between utilized  
 modulation and occupied spectrum of PostSplitLightpaths.

#### 2) Optical-Layer Constraints for Newly-Setup Lightpaths:

$$-M \cdot (\chi_f^{(\tilde{i}, \tilde{j})} - \chi_{f+1}^{(\tilde{i}, \tilde{j})} - 1) \geq \sum_{f' \in [f+2, W]} \chi_{f'}^{(\tilde{i}, \tilde{j})}, \\ \forall \tilde{i}, \tilde{j} \in \mathbf{N}, f \in [1, F-1]. \quad (19) \quad 445$$

$$\sum_{n \in \mathbf{N}} \lambda_{(m,n),f}^{(\tilde{i},\tilde{j})} - \sum_{n \in \mathbf{N}} \lambda_{(n,m),f}^{(\tilde{i},\tilde{j})} = \begin{cases} \chi_f^{(\tilde{i},\tilde{j})}, & m = \tilde{i} \\ -\chi_f^{(\tilde{i},\tilde{j})}, & m = \tilde{j} \\ 0, & m \neq \tilde{i}, \tilde{j}, \end{cases} \quad \forall f \in [1, F], \tilde{i}, \tilde{j} \in \mathbf{N}. \quad (20)$$

$$\sum_{l \in \mathbf{L}, x, y \in \mathbf{N}} \xi_{(m,n),f}^{l,(x,y)} + \sum_{\tilde{i}, \tilde{j} \in \mathbf{N}} \lambda_{(m,n),f}^{(\tilde{i},\tilde{j})} \leq 1, \quad \forall f \in [1, F], (m, n) \in \mathbf{E}. \quad (21)$$

$$\sigma_{(m,n)}^{(\tilde{i},\tilde{j})} \leq \sum_{f \in [1, F]} \lambda_{(m,n),f}^{(\tilde{i},\tilde{j})} \leq \sigma_{(m,n)}^{(\tilde{i},\tilde{j})} \cdot M, \quad \forall \tilde{i}, \tilde{j} \in \mathbf{N}, (m, n) \in \mathbf{E}. \quad (22)$$

$$\sum_{n \in \mathbf{N}} \sigma_{(m,n)}^{(\tilde{i},\tilde{j})} \leq 1, \quad \forall \tilde{i}, \tilde{j}, m \in \mathbf{N}. \quad (23)$$

$$\sum_{m \in \mathbf{N}} \sigma_{(m,n)}^{(\tilde{i},\tilde{j})} \leq 1, \quad \forall \tilde{i}, \tilde{j}, n \in \mathbf{N}. \quad (24)$$

$$\sigma_{(m,n)}^{(\tilde{i},\tilde{j})} + \sigma_{(n,m)}^{(\tilde{i},\tilde{j})} \leq 1, \quad \forall \tilde{i}, \tilde{j}, (m, n) \in \mathbf{E}. \quad (25)$$

$$\sum_{a \in \mathbf{A}} \theta_a^{(\tilde{i},\tilde{j})} \leq 1, \quad \forall \tilde{i}, \tilde{j} \in \mathbf{N}. \quad (26)$$

$$\sum_{(m,n) \in \mathbf{E}} \lambda_{(m,n),f}^{(\tilde{i},\tilde{j})} \cdot D(m, n) \leq T(a) - M \cdot (\theta_a^{(\tilde{i},\tilde{j})} - 1), \quad \forall \tilde{i}, \tilde{j} \in \mathbf{N}, f \in [1, F], a \in \mathbf{A}. \quad (27)$$

$$\sum_{a \in \mathbf{A}} \theta_a^{(\tilde{i},\tilde{j})} \leq \sum_{f \in [1, F]} \chi_f^{(\tilde{i},\tilde{j})} \leq M \cdot \sum_{a \in \mathbf{A}} \theta_a^{(\tilde{i},\tilde{j})}, \quad \forall \tilde{i}, \tilde{j} \in \mathbf{N}. \quad (28)$$

Eq. (19) ensures lightpaths' occupied spectrum slots should be consecutive. Eq. (20) is optical-layer flow-conservation constraint. Eq. (21) ensures a spectrum slot on a fiber can only be used once. Eq. (22) ensures that a fiber link is used when spectrum slots on this fiber are used. Eqs. (23)-(25) ensure that lightpaths are routed without loops. Eq. (26) ensures a lightpath adopts only one modulation format, and Eq. (27) is lightpaths' maximum transmission reach constraint. Eq. (28) formulates the relationship between utilized modulation and occupied spectrum of a lightpath.

3) *Electrical-Layer Constraints for Traffic Spikes*: Traffic spikes are provisioned over incremental network configurations, which are the combination of UnSplitLightpaths, PostSplitLightpaths and Newly-Setup Lightpaths, as depicted in Fig. 4. Therefore,  $(i, j)$  here represents the sum of all lightpaths capacities from node  $i$  to node  $j$ .

$$\sum_{j \in \mathbf{N}} \alpha_{(i,j)}^r - \sum_{j \in \mathbf{N}} \alpha_{(j,i)}^r = \begin{cases} \varepsilon_r, & i = s_r \\ -\varepsilon_r, & i = d_r \\ 0, & i \neq s_r, d_r, \end{cases} \quad \forall r \in \mathbf{R}. \quad (29)$$

$$\sum_{i \in \mathbf{N}} \alpha_{(i,j)}^r \leq 1, \quad \forall r \in \mathbf{R}, j \in \mathbf{N}. \quad (30)$$

$$\sum_{j \in \mathbf{N}} \alpha_{(i,j)}^r \leq 1, \quad \forall r \in \mathbf{R}, i \in \mathbf{N}. \quad (31)$$

$$\alpha_{(i,j)}^r + \alpha_{(j,i)}^r \leq 1, \quad \forall r \in \mathbf{R}, i, j \in \mathbf{N}. \quad (32)$$

$$\rho_r \leq \mu \cdot b_r, \quad \forall r \in \mathbf{R}. \quad (33)$$

$$\varepsilon_r \leq \rho_r \leq M \cdot \varepsilon_r, \quad \forall r \in \mathbf{R}. \quad (34)$$

$$\sum_{r \in \mathbf{R}} \rho_r \cdot \alpha_{(i,j)}^r + \sum_{l \in \mathbf{L}} B(l) \cdot \pi_{(i,j)}^l \leq C \cdot \sum_{f \in [1, F]} \sum_{a \in \mathbf{A}}$$

TABLE I  
MODULATION FORMAT VS. DATA RATE VS. TRANSMISSION REACH

Modulation format	BPSK	QPSK	8QAM	16QAM
Bits per symbol (b/s/Hz)	1	2	3	4
Slot bandwidth (GHz)	12.5	12.5	12.5	12.5
Data rate (Gbps)	12.5	25	37.5	50
Transmission reach (km)	9600	4800	2400	1200

$$\left( \sum_{l \in \mathbf{L}} \varphi_{(i,j),f}^l \cdot a \cdot \omega_{(i,j),a}^l + \chi_f^{(i,j)} \cdot a \cdot \theta_a^{(i,j)} \right), \quad \forall i, j \in \mathbf{N}. \quad (35)$$

Eq. (29) is electrical-layer flow-conservation constraint. Eqs. (30)-(32) ensure that lightpaths are routed over a single path on optical layer without loops. Eq. (33) ensures that the actual access bandwidth should not exceed the original requested bandwidth. Eq. (34) shows when traffic is blocked. Eq. (35) is lightpath capacity constraint ensuring that the sum of served bandwidth of traffic spikes and baseline traffic can not exceed the sum capacity of UnSplitLightpaths, PostSplitLightpaths, and newly-setup lightpaths between node pair  $(i, j)$ .

### B. Model Linearization and Optimization Results

For non-linear constraints Eqs. (12), (35), we linearize them with auxiliary variables and constraints added.<sup>6,7</sup>

A relative small-scale 6-node topology (as shown in Fig. 5(a)) is adopted to evaluate the performance of our proposed optimization model. We run our optimization model by a commercial IBM CPLEX solver on a computer with 2.4 GHz CPU and 32 GB RAM.<sup>8</sup> All fibers are unidirectional with 20 spectrum slots, and width of each slot is 12.5 GHz.

On the input parameters, Table I summarizes the parameters of different modulation formats according to theoretical and experimental results that have demonstrated the tradeoff between transmission reach and modulation level [26], [52]–[57]. Table II shows the input traffic profile as well as configurations of baseline lightpaths. Under the condition that all baseline traffic is served, we start with low modulation levels first, and increase modulation levels as the amount of traffic spike increases before lightpath splitting. Note also that the effectiveness of lightpath splitting does not rely on these specific data. As long as the two prerequisites in Section III.D can be satisfied, similar performance can be yielded.

Two benchmark experiments are conducted as comparisons. One is named *all lightpath splitting*, which means that all intermediate nodes of baseline lightpaths are set to be SplitPoints. The other is called *without lightpath splitting*, which means lightpath splitting is not performed, and the traffic spikes is

<sup>6</sup>Linearization for the product  $c$  of two binary variables  $a, b$ .  $c$  is also a binary variable,  $c = a \cdot b$ , subject to:  $c \geq a + b - 1$ ,  $c \leq a$ ,  $c \leq b$ .

<sup>7</sup>Linearization for the product of a binary variable  $x$  and a integer variable  $y$ : we assume that  $y$  has a set of its possible integer values  $Y = \{w_i\}$  ( $1 \leq i \leq n_Y$ ), where  $w_i$  is a parameter, and  $n_Y$  is the size of  $Y$ . Then, we define a binary variable  $z_i$ , subject to:  $y = w_i \cdot z_i$ ,  $\forall i \in [1, n_Y]$ . Therefore, the product,  $x \cdot y$  can be expressed as the product of two binary variables, thus it can be further linearized with the method in footnote 6.

<sup>8</sup>Not all runs finished their optimization, so we further set a maximum running time of 72 hours, and a relative gap tolerance of 0.01 between best integer and best bound in the solver. The solver will finish its calculation and return results if either criterion is reached.

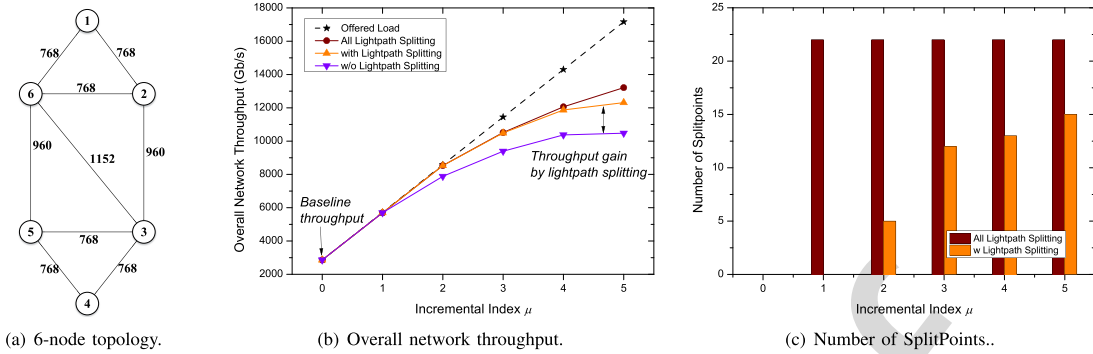


Fig. 5. Optimization topology and results.

TABLE II

INPUTS: BASELINE LIGHTPATHS CONFIGURATIONS AND BASELINE TRAFFIC PROFILE (TOTAL AMOUNT = 2861 Gb/s)

Baseline Lightpaths $l$	$S(l)$ (b/s/Hz)	$W(l)$ (GHz)	$B(l)$ (Gb/s)	Supporting requests $r$
(1,2)	2	112.5	185	(1,2,185)
(1,6,3)	1	112.5	103	(1,3,103)
(1,6,3,5,4)	1	50	47	(1,4,47)
(1,6,5)	1	87.5	71	(1,5,71)
(1,2,3,6)	2	100	195	(1,6,195)
(2,1)	1	162.5	155	(2,1,155)
(2,3)	1	100	93	(2,3,93)
(2,3,4)	1	37.5	37	(2,4,37)
(2,6,5)	1	37.5	24	(2,5,24)
(2,6)	1	137.5	130	(2,6,130)
(3,2,1)	1	37.5	33	(3,1,33)
(3,2)	1	12.5	2.5	(3,2,2.5)
(3,4)	1	200	151	(3,4,151)
(3,5)	1	200	174	(3,5,174)
(3,2,6)	1	50	39	(3,6,39)
(4,5,6,1)	2	100	192	(4,1,192)
(4,3,2)	1	50	45	(4,2,45)
(4,3)	1	187.5	181	(4,3,181)
(4,5)	1	87.5	81	(4,5,81)
(4,5,3,6)	2	62.5	114	(4,6,114)
(5,6,2,1)	1	37.5	32	(5,1,32)
(5,6,2)	1	100	98	(5,2,98)
(5,3)	1	125	122	(5,3,122)
(5,4)	1	162.5	153	(5,4,153)
(5,3,6)	1	50	45	(5,6,45)
(6,1)	1	150	124	(6,1,124)
(6,2)	1	100	88	(6,2,88)
(6,3)	1	50	46	(6,3,46)
(6,5,3,4)	1	12.5	12.5	(6,4,12.5)
(6,5)	1	112.5	88	(6,5,88)

served by new lightpath establishment and baseline lightpaths modulation adjustments if baseline lightpaths are not using highest-possible modulations.

Fig. 5(b) numerically depicts the performance on overall network throughput. Even without lightpath splitting, there is still room for an increase of network throughput. This improvement is possible as the baseline traffic is usually served with a certain amount of excess capacity (in both electrical and optical layers), and part of the spikes can be accepted by raising modulation levels of existing lightpaths, establishing new lightpaths using spare spectrum, and grooming onto existing lightpaths with spare electrical-layer bandwidth. Besides, we can also observe that *with lightpath splitting* can achieve similar performance as *all lightpath splitting*. The reason is that, during traffic fluctuations, some network links are under resource crunch, while some other links may

still have spare capacity, this leads to the result that not all lightpaths need to be split. The results in Table III also support this point. The gap between *with lightpath splitting* and *all lightpath splitting* is due to the fact that the ILP did not finished its optimization within reasonable time (see footnote 8).

Fig. 5(c) shows the number of SplitPoints (number of added transceiver pairs) returned by the optimization model as traffic load increases. As expected, more SplitPoints are activated to accommodate incremental traffic spikes as load increases. Combining Figs. 5(b) and 5(c), an important message is that, by wisely selecting SplitPoints, lightpath splitting can achieve almost the same throughput as setting all intermediate nodes as SplitPoints (*all lightpath splitting*), while reducing the number of SplitPoints to mitigate impacts on existing traffic.

Table III shows the details of how SplitLightpaths are split into PostSplitLightpaths. We conclude that lightpaths with higher load tend to be selected as SplitLightpaths. As the load of traffic spike increases, more SplitLightpaths are involved.

C. Complexity Analysis

Table IV shows the problem size of the mathematical formulation. On time complexity, as our lightpath splitting problem involves lightpaths splitting decision and corresponding RMSA, as well as new lightpaths RMSA, it is more complex than classical RSA problems, which has been proved to be NP-hard [58]. Therefore, our problem is NP-hard.

V. SCALABLE ALGORITHMS FOR LIGHTPATH SPLITTING

The mathematical optimization can process all traffic requests and return the whole network configurations after lightpath splitting simultaneously, but it has high computational complexity. To design scalable algorithms, we follow the divide-and-conquer rule for quickly solving the problem.

For baseline traffic accommodation, we try to minimize number of used transceivers (the MinLP policy in [59]). The modulation level is assigned following the practical principle that highest-possible modulation level is used [60]. Traffic requests are served in descending order of requested bandwidth.

A. Divide-and-Conquer Problem Decomposition

Similar to designing a multi-layer optical network [61], the problem of lightpath splitting can be partitioned into the following subproblems (which are not necessarily independent):

- 1) *Decide the Number of SplitPoints on Baseline Lightpaths*: determine the number ( $K$ ) of SplitPoints (also the number of added transceiver pairs) on baseline configurations.

TABLE III  
OPTIMIZATION RESULTS: UNSPLITLIGHTPATHS, SPLITLIGHTPATHS, POSTSPLITLIGHTPATHS AND LIGHTPATH LOAD

UnsplitLightpaths*	Load (Gb/s)	Possible SplitLightpaths	Load (Gb/s)	PostSplitLightpaths**				
				$\mu = 1$	$\mu = 2$	$\mu = 3$	$\mu = 4$	$\mu = 5$
(5,3,6)	45	(1,2,3,6)	195	(1,2,3,6)	<b>(1,2), (2,3,6)</b>	<b>(1,2), (2,3,6)</b>	<b>(1,2), (2,3), (3,6)</b>	<b>(1,2), (2,3), (3,6)</b>
(3,2,6)	39	(4,5,6,1)	192	(4,5,6,1)	<b>(4,5), (5,6,1)</b>	<b>(4,5), (5,6,1)</b>	<b>(4,5), (5,6), (6,1)</b>	<b>(4,5), (5,6), (6,1)</b>
(2,3,4)	37	(4,5,3,6)	114	(4,5,3,6)	<b>(4,5,3), (3,6)</b>	<b>(4,5), (5,3), (3,6)</b>	<b>(4,5), (5,3), (3,6)</b>	<b>(4,5), (5,3), (3,6)</b>
(2,6,5)	24	(1,6,3)	103	(1,6,3)	<b>(1,6), (6,3)</b>	<b>(1,6), (6,3)</b>	<b>(1,6), (6,3)</b>	<b>(1,6), (6,3)</b>
		(5,6,2)	98	(5,6,2)	(5,6,2)	<b>(5,6), (6,2)</b>	(5,6,2)	(5,6,2)
		(1,6,5)	71	(1,6,5)	(1,6,5)	<b>(1,6), (6,5)</b>	<b>(1,6), (6,5)</b>	<b>(1,6), (6,5)</b>
		(1,6,3,5,4)	47	(1,6,3,5,4)	(1,6,3,5,4)	<b>(1,6), (6,3,5,4)</b>	<b>(1,6), (6,3), (3,5), (5,4)</b>	<b>(1,6), (6,3,5), (5,4)</b>
		(4,3,2)	45	(4,3,2)	(4,3,2)	<b>(4,3), (3,2)</b>	<b>(4,3), (3,2)</b>	<b>(4,3), (3,2)</b>
		(3,2,1)	33	(3,2,1)	(3,2,1)	(3,2,1)	(3,2,1)	(3,2,1)
		(5,6,2,1)	32	(5,6,2,1)	<b>(5,6,2), (2,1)</b>	<b>(5,6), (6,2,1)</b>	<b>(5,6), (6,2,1)</b>	<b>(5,6,2), (2,1)</b>
		(6,5,3,4)	12.5	(6,5,3,4)	(6,5,3,4)	<b>(6,5), (5,3), (3,4)</b>	(6,5,3,4)	<b>(6,5), (5,3), (3,4)</b>

\* One-hop lightpaths that traverse no intermediate nodes on optical layer are not shown here. They also belong to the category of UnsplitLightpaths.

\*\* For each  $\mu$ , only bolder ones refer to PostSplitLightpaths, while normal ones are UnsplitLightpaths.

TABLE IV  
SIZE OF FORMULATIONS FOR LIGHTPATH SPLITTING

Variables	$\mathcal{O}( \mathbf{L}  \mathbf{N} ^2 \mathbf{E} F +  \mathbf{L}  \mathbf{N} ^2 \mathbf{A}  +  \mathbf{R}  \mathbf{N} ^2)$
Constraints	$\mathcal{O}( \mathbf{L}  \mathbf{N} ^2 \mathbf{E} F +  \mathbf{L}  \mathbf{N} ^2 \mathbf{A} F +  \mathbf{R}  \mathbf{N} ^2 +  \mathbf{N} ^3)$

2) Which Lightpath and How to Split the Lightpath: determine which baseline lightpaths to be split, and how to split each lightpath.

3) PostSplitLightpaths Resource Allocation: remove SplitLightpaths and allocate spectrum to PostSplitLightpaths.

4) Incremental Traffic Routing After Lightpath Splitting: setup new lightpaths if necessary, and route incremental traffic on the network consisting of un-split baseline lightpaths, PostSplitLightpaths, and newly-setup lightpaths.

The heuristic cannot solve the four subproblems as a whole. So, we transform subproblem 1 into a decisive variable input, controlling how many lightpath-splitting operations are executed in network. When the number of SplitPoints,  $K$ , is set to be a controlled variable, subproblem 2 can be transformed into a simpler one, i.e., the *lightpath-SplitPoint-selection problem*, which is the goal for heuristic design. Subproblems 3, 4 act as post-split operations, which will be discussed in Section V.D.

Finally, the logical flow for using heuristic algorithms to solve the lightpath splitting problem is: 1) when traffic spikes first arrive, part of the spikes can be accepted by the network using spare capacities. 2) As this gap is filled up to compose an extended baseline network configuration, lightpath splitting is triggered. At this stage, we should first decide the number of SplitPoints. 3) Then, we should determine the distribution of these SplitPoints on the extended baseline network configuration, and how to allocate spectrum to the PostSplitLightpaths. 4) Finally, we route the rest of the traffic spikes on this network configuration by both grooming [59], [62] onto existing lightpaths, or setting up new lightpaths. To maximize network throughput, all traffic requests are served one by one following a descending order of requested bandwidth based on multi-layer auxiliary graphs [59], [63].

### B. Pre-Splitting Preparations

When incremental traffic spikes arrive, we first use Algorithm 1 to accommodate as many requests as possible before lightpath splitting using spare capacity in both optical and electrical layers. This is also the normal operation for

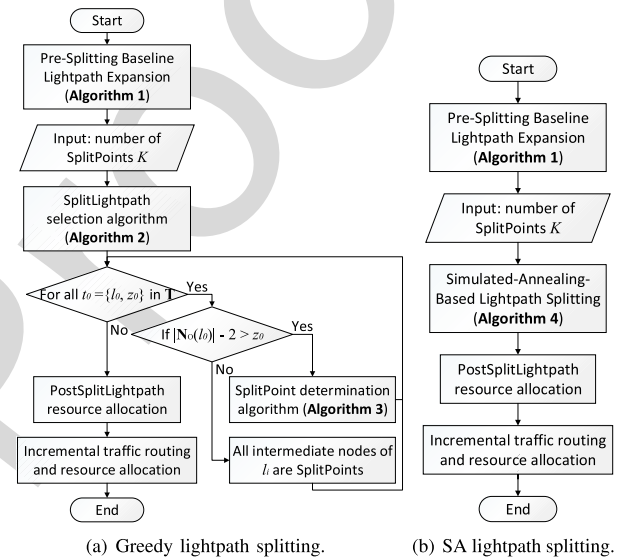


Fig. 6. Flowchart for different lightpath-splitting algorithms.

networks without lightpath splitting when traffic spikes arrive. Lightpath splitting is triggered when there is not enough capacity for serving more traffic. The network configuration at this time is the starting point for lightpath splitting.

### C. Solving the Lightpath-SplitPoint-Selection Problem

Formally, given a network topology  $\mathbf{G}(\mathbf{N}, \mathbf{E})$ , the *lightpath-SplitPoint-selection problem* is to find  $K$  SplitPoints on all existing lightpaths possible to be split. We try both greedy and Simulated-Anneal (SA) methods to solve the problem.

1) *Greedy Lightpath Splitting*: In greedy lightpath splitting algorithm, we concentrate on which lightpaths, i.e., SplitLightpaths, to split (solved by Algorithm 2: SplitLightpaths selection), and where to split along the lightpath (solved by Algorithm 3: SplitPoints determination). The execution flowchart of the two algorithms can be found in Fig. 6(a).

#### • Which Lightpath to Split?

According to Definition 1-3, we define a SplitLightpaths set  $\mathbf{T}$  consisting of tuples:  $t_i = [l_i, z_i]$ , which represents that SplitLightpath  $l_i$  is to be split  $z_i$  times into  $z_i + 1$  PostSplitLightpaths by  $z_i$  SplitPoints  $\mathbf{V}_{l_i} = \{[v_1, l_i], [v_2, l_i], \dots, [v_{z_i}, l_i]\}$ ,  $v_1, v_2, \dots, v_{z_i} \in \mathbf{N}_O(l_i)$ .



---

**Algorithm 1** Baseline Lightpath Expansion (also performs as w/o *Lightpath Splitting*)

---

**Input:** baseline network configurations with baseline lightpaths set  $\mathbf{L}$ ; incremental traffic profile  $\mathbf{R}_I$ ;  
**Output:** expanded baseline lightpaths set  $\mathbf{L}_E$ ; incremental traffic residual profile  $\mathbf{R}_{I,r}$ ;

- 1: sort all incremental traffic  $\tilde{r} \in \mathbf{R}_I$  in descending order of bandwidth  $\tilde{b}_{\tilde{r}}$ ;
- 2:  $\mathbf{L}_E \leftarrow \mathbf{L}$
- 3: **for**  $i = 0$  to  $|\mathbf{R}_I|$  **do**
- 4: route  $\tilde{r}_i$  with maximum bandwidth possible ( $\tilde{b}_{\tilde{r},m}$ ) on baseline network configurations using multi-layer auxiliary graph model [63], and add the new lightpath into  $\mathbf{L}_E$ ; the unserved bandwidth ( $\tilde{b}_{\tilde{r}} - \tilde{b}_{\tilde{r},m}$ ) of each request forms  $\mathbf{R}_{I,r}$ ;
- 5: **end for**

---

Basically, previous optimization results in Table III reveal that lightpaths under larger load tend to be split earlier. Then, we follow this thread to design Algorithm 2. Inspired by strategies of breadth-first or depth-first search algorithms, we introduce two greedy options to either set at least one SplitPoint per SplitLightpath so as to split as many lightpaths as possible (BF: Breath First), or set as many SplitPoints as possible on the SplitLightpaths to split lightpaths harder (DF: Depth First).<sup>9</sup>

- *How to Split the selected SplitLightpaths?*

When Algorithm 2 returns the SplitLightpaths set  $\mathbf{T}$ , we further apply Algorithm 3 to determine the exact SplitPoints on SplitLightpaths. In Algorithm 3, we further evaluation two greedy options: either to maximize electrical-layer capacity by adjusting modulation level without shrinking occupied spectrum (MaxE), or to maximize optical-layer available resources by adjusting modulation level while shrinking occupied spectrum (MaxO), as first introduced in Section III.A.

Finally, by combining the two policies on which lightpath to split and the two policies on how to split the selected SplitLightpaths, we introduce four policies for greedy lightpath splitting: BF-MaxE, DF-MaxE, BF-MaxO, and DF-MaxO.

2) *Simulated-Annealing (SA)-Based Lightpath Splitting:* In this section, we define a basic operation, *SplitPoint exchange* (inspired by node-exchange [61] and branch-exchange [64]), for designing a lightpath-splitting algorithm based on SA.

**Definition 4:** In a *SplitPoint-exchange* operation, a SplitPoint inside the candidate set is swapped with other SplitPoint outside the candidate set. Mathematically, there is a set  $\mathbf{V}$  comprises all possible SplitPoints (represented by  $V_i = [v, l]$ ). Then, we have a candidate SplitPoint set  $\mathbf{V}_c$  with  $|\mathbf{V}_c| = K$  elements,  $\mathbf{V}_c \subseteq \mathbf{V}$ . Randomly select  $\forall V_i \in \mathbf{V}_c, V_j \in \mathbf{V} \setminus \mathbf{V}_c$ , delete  $V_i$  from  $\mathbf{V}_c$ , while put  $V_j$  into  $\mathbf{V}_c$  to form a new  $\mathbf{V}_c'$ .

For such a SplitPoint exchange, neighboring configurations  $\mathbf{V}_c'$  that returns better results (higher network throughput  $Y$ ) than original configurations (baseline network throughput  $Y_0$ )  $\mathbf{V}_c$  will be accepted. Meanwhile, those whose outputs after the SplitPoint-exchange operation are worse than the initial state

<sup>9</sup>It should be noted that, as  $K$  grows larger, BF and DF policies will finally converge with *all lightpath splitting* policy, as all possible intermediate nodes are selected as SplitPoints.

---

**Algorithm 2** Greedy SplitLightpaths Selection

---

**Input:** number of SplitPoints  $K$ ; expanded baseline lightpaths set  $\mathbf{L}_E$ ; incremental traffic residual profile  $\mathbf{R}_{I,r}$ ; *greedy options:* breadth first ( $g_1 = 0$ ) or depth first ( $g_1 = 1$ );

**Output:** SplitLightpaths set  $\mathbf{T}$ ;

- 1: construct a virtual topology  $\mathbf{G}'(\mathbf{N}, \mathbf{L}_E \cup \mathbf{E})$  consisting of  $\mathbf{N}$  nodes, and lightpaths in  $\mathbf{L}_E$  as edges with infinite capacity, and available optical resources as edges with actual optical capacity;
- 2: **for**  $j = 1$  to  $|\mathbf{R}_{I,r}|$  **do**
- 3: route residual bandwidth of  $\tilde{r}_j$  on  $\mathbf{G}'$ ;
- 4: **end for**
- 5: sort lightpath  $l_i \in \mathbf{L}_E$  in descending order of bandwidth;
- 6: **if**  $g_1 = 0$  **then**
- 7: **for**  $k = 1$  to  $K$  **do**
- 8: **if**  $|\mathbf{N}_O(l_k)| > 2$  **then**
- 9: add  $[l_k, 1]$  into  $\mathbf{T}$ ;
- 10: **end if**
- 11: **end for**
- 12: **if**  $|\mathbf{T}| < K$  **then**
- 13:  $t \leftarrow 1$ ;
- 14: **while**  $t < K - |\mathbf{T}|$  **do**
- 15: **if**  $|\mathbf{N}_O(l_k)| - 2 > K - |\mathbf{T}| - t$  **then**
- 16: revise  $[l_t, 1]$  to be  $[l_t, K - |\mathbf{T}| - t]$ ;
- 17:  $t \leftarrow K - |\mathbf{T}|$ ;
- 18: **else**
- 19: revise  $[l_t, 1]$  to be  $[l_t, |\mathbf{N}_O(l_k)| - 2]$ ;
- 20:  $t \leftarrow t + |\mathbf{N}_O(l_k)| - 2$ ;
- 21: **end if**
- 22: **end while**
- 23: **end if**
- 24: **else**
- 25:  $k \leftarrow 1$ ;
- 26: **while**  $k < K$  **do**
- 27: **if**  $|\mathbf{N}_O(l_k)| - 2 > K - k$  **then**
- 28: add  $[l_k, K - k]$  into  $\mathbf{T}$ ;
- 29:  $k \leftarrow K$ ;
- 30: **else**
- 31: add  $[l_k, |\mathbf{N}_O(l_k)| - 2]$  into  $\mathbf{T}$ ;
- 32:  $k \leftarrow k + |\mathbf{N}_O(l_k)| - 2$ ;
- 33: **end if**
- 34: **end while**
- 35: **end if**

---

are accepted with a variable acceptance probability  $\vartheta$  lying on the “system temperature”  $\tau$ , which is gradually decreasing as the algorithm progresses to simulate the annealing process. The algorithm will terminate when  $\tau$  reaches the “ending temperature”  $\tau_e$ , and returns results, where:

$$\vartheta = \begin{cases} 1, & Y \geq Y_0 \\ \exp\left(-\frac{Y_0 - Y}{\tau}\right), & Y < Y_0 \end{cases} \quad (36)$$

The SA-based lightpath splitting (algorithm 4) method can return the SplitPoint set  $\mathbf{V}$  directly. However, the remaining unsolved problem is how to allocate spectrum for PostSplitLightpaths. Then, we combine the previously dis-

**Algorithm 3** Greedy SplitPoints Determination

---

**Input:** a SplitLightpath  $t_0 = [l_0, z_0]$ , number of occupied spectrum slots  $W(l_0)$ , and modulation level  $S(l_0)$ ;  
*greedy options:* MaxE ( $g_2 = 0$ ) or MaxO ( $g_2 = 1$ );  
**Output:** SplitPoint set  $\mathbf{V}(l_0) = \{[v_1, l_0], [v_2, l_0], \dots, [v_{z_0}, l_0]\}$  for SplitLightpaths  $t_0 = [l_0, z_0]$ ;

- 1: sum of electrical-layer capacity  $Q \leftarrow 0$ ; sum of occupied spectrum slots  $U \leftarrow \infty$ ;
- 2: **for** all possible  $\{v_1, v_2, \dots, v_{z_0}\} \subsetneq \mathbf{N}_O(l)$  **do**
- 3: lightpath  $l_0$  is split into  $z_0 + 1$  segments:  $l_1, l_2, \dots, l_{z_0+1}$ ;
- 4: raise  $S(l_1), S(l_2), \dots, S(l_{z_0+1})$  to the maximum possible;
- 5: **if**  $g_2 = 0$  **then**
- 6:  $Q_i \leftarrow \sum_{1 \leq k \leq z_0+1} W(l_k)S(l_k)$ ;
- 7: **if**  $Q_i > Q$  **then**
- 8:  $\mathbf{V}(l_0) \leftarrow \{[v_1, l_0], [v_2, l_0], \dots, [v_{z_0}, l_0]\}$ ;
- 9: **end if**
- 10: **else**
- 11: shrink  $W(l_1^i), W(l_2^i), \dots, W(l_{z_0}^i)$  to the minimum possible;
- 12:  $U_i \leftarrow \sum_{1 \leq k \leq z_0+1} W(l_k)$ ;
- 13: **if**  $U_i < U$  **then**
- 14:  $\mathbf{V}(l_0) \leftarrow \{[v_1, l_0], [v_2, l_0], \dots, [v_{z_0}, l_0]\}$ ;
- 15: **end if**
- 16: **end if**
- 17: **end for**

---

686 cussed policies (MaxE and MaxO) with SA, and introduce  
 687 two policies: SA-MaxE and SA-MaxO.

688 *D. Post-Splitting Configurations*

689 As shown in Fig. 6, post-splitting network configurations,  
 690 i.e., lightpath splitting resource allocation and incremental traf-  
 691 fic accommodation, should be executed after deciding which  
 692 and how to split lightpaths. For MaxE policies, spectrum allo-  
 693 cation is not changed. For MaxO policies, we use a First-Fit  
 694 strategy to reassign shrunken spectrum slots with smaller  
 695 index to reduce spectrum fragmentation. On incremental traffic  
 696 accommodation, we still use the multi-layer auxiliary graph  
 697 network model as of baseline traffic [59], [63].

698 *E. Complexity Analysis*

699 1) *Greedy Lightpath Splitting:* Greedy lightpath splitting  
 700 scheme first determines SplitLightpaths (Algorithm 2) with  
 701 the complexity of  $\mathcal{O}(|\mathbf{R}_{\mathbf{I},\mathbf{r}}| |\mathbf{N}|^2 + |\mathbf{L}_{\mathbf{E}}|^2 + K)$ . Then, there is  
 702 a loop for executing Algorithm 3 to split each lightpaths in  $\mathbf{T}$ .  
 703 In Algorithm 3, for each SplitLightpath  $t_0 = [l_0, z_0]$ , there are  
 704  $\binom{|\mathbf{N}_O(l_0)|-2}{z_0}$  possible  $\{v_1, v_2, \dots, v_{z_0}\}$  from  $\mathbf{N}_O(l_0)$ , based  
 705 on principles of combinatorial number. In lightpath splitting  
 706 resource allocation, at most  $2K$  PostSplitLightpaths will use  
 707 first fit to try at most  $F$  slots to reallocate spectrum resource,  
 708 resulting in a complexity of  $\mathcal{O}(KF)$ . While in incremental  
 709 traffic accommodation, the size of auxiliary graph is  $(F +$   
 710  $1)|\mathbf{N}|$  [63]. The complexity of running Dijkstra for RSA  
 711 is  $\mathcal{O}(|\mathbf{N}|^2 F^2)$ . So, the total complexity is  $\mathcal{O}(|\mathbf{R}_{\mathbf{I},\mathbf{r}}| |\mathbf{N}|^2 +$   
 712  $|\mathbf{L}_{\mathbf{E}}|^2 + K) + \mathcal{O}(|\mathbf{T}| \binom{|\mathbf{N}_O(l_0)|-2}{z_0}) + \mathcal{O}(KF) + \mathcal{O}(|\mathbf{N}|^2 F^2)$ .

713 As the number of SplitLightpaths is no larger than the  
 714 number of SplitPoints,  $|\mathbf{T}| \leq K$ . The number of incremental

**Algorithm 4** SA-Based Lightpath Splitting

---

**Input:** number of SplitPoints  $K$ ; expanded baseline light-  
 paths set  $\mathbf{L}_{\mathbf{E}}$ ; incremental traffic residual profile  $\mathbf{R}_{\mathbf{I},\mathbf{r}}$ ; SA  
 initial temperature  $\tau_0$ , ending temperature  $\tau_e$ , and cooling  
 parameter  $\gamma$ ;  
**Output:** SplitPoint set  $\mathbf{V} = \{\mathbf{V}_{l_0}, \mathbf{V}_{l_1}, \dots, \mathbf{V}_{l_n}\}$

- 1:  $\tau \leftarrow \tau_0$ ;
- 2: randomly select  $K$  SplitPoints, and put them into  $\mathbf{V}_{\mathbf{c}}$ ;
- 3: lightpath splitting resource allocation; incremental traffic  
 routing and resource allocation;  $Y_0 \leftarrow$  current network  
 throughput;
- 4: **while**  $\tau > \tau_e$  **do**
- 5: randomly select  $V_i \in \mathbf{V}_{\mathbf{c}}, V_j \in \mathbf{V} \setminus \mathbf{V}_{\mathbf{c}}$ , and perform  
 SplitPoint exchange;
- 6: lightpath splitting resource allocation; incremental traffic  
 routing and resource allocation;  $Y \leftarrow$  current network  
 throughput;
- 7: **if**  $\vartheta > \text{random}(0,1)$  **then**
- 8: delete  $V_i$  from  $\mathbf{V}_{\mathbf{c}}$ , put  $V_j$  into  $\mathbf{V}_{\mathbf{c}}$  to form a new  $\mathbf{V}_{\mathbf{c}}$ ';
- 9: **end if**
- 10: cooling the annealing temperature  $\tau \leftarrow \tau \cdot \gamma$ ;
- 11: **end while**

---

traffic residual requests between node pairs should be no larger  
 than the square of node number,  $|\mathbf{R}_{\mathbf{I},\mathbf{r}}| \leq |\mathbf{N}|^2$ . The number  
 of expanded baseline lightpaths should be no larger than the  
 number of spectrum slots times the square of node number,  
 $|\mathbf{L}_{\mathbf{E}}| \leq F|\mathbf{N}|^2$ . For BF policies,  $z_0 = 1$ ,  $\binom{|\mathbf{N}_O(l_0)|-2}{1} =$   
 $|\mathbf{N}_O(l_0)| - 2 < |\mathbf{N}|$ . For DF policies,  $z_0 = |\mathbf{N}_O(l_0)| - 2$   
 is true in most lightpaths,  $\binom{|\mathbf{N}_O(l_0)|-2}{|\mathbf{N}_O(l_0)|-2} = 1$ . While there is  
 only one possible lightpath that  $1 \leq z_0 \leq |\mathbf{N}_O(l_0)| - 2$ . The  
 number of nodes a lightpath traverses should be no larger than  
 the total number of nodes, so,  $\binom{|\mathbf{N}_O(l_0)|-2}{z_0} < \binom{|\mathbf{N}|}{z_0} \sim |\mathbf{N}|^{z_0}$ .  
 The final complexity is  $\mathcal{O}(F^2 |\mathbf{N}|^4 + K |\mathbf{N}|^{z_0} + KF)$ .

2) *SA-Based Lightpath Splitting:* The complexity of SA is  
 related to SA initial temperature  $\tau_0$ , ending temperature  $\tau_e$ ,  
 and cooling parameter  $\gamma$ . In our algorithm, there is a loop  
 controlled by current temperature  $\tau$ . The execution times  $\kappa$  of  
 this loop can be determined as follows:

$$\tau_0 \cdot \gamma^{\kappa-1} > \tau_e > \tau_0 \cdot \gamma^{\kappa} \quad (37)$$

On each  $\tau$ , a SplitPoint-exchange operation and current  
 throughput calculation are performed. As analyzed before,  
 the complexity of lightpath splitting resource allocation and  
 incremental traffic accommodation is  $\mathcal{O}(F^2 |\mathbf{N}|^2)$ . The final  
 complexity is  $\mathcal{O}(\kappa F^2 |\mathbf{N}|^2)$ .

## VI. ILLUSTRATIVE NUMERICAL EXAMPLES

## A. Simulation Setup

In this section, we implement the proposed algorithms  
 by a network simulator developed on C++ to evaluate the  
 performance of lightpath splitting. We use NSFNET backbone  
 topology (modified to avoid crosslinks, Fig. 7). All fibers  
 are unidirectional with 30 spectrum slots, and the spectrum  
 width of each slot is 12.5 GHz. Each node is equipped with  
 enough transceivers for lightpath splitting as we analyzed  
 before in Assumption 1. For each simulation run, the traffic

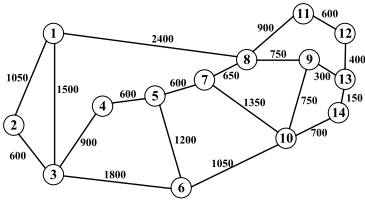
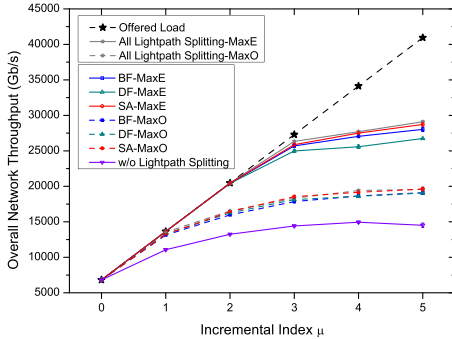


Fig. 7. NSFNET network topology (14 nodes, 20 bidirectional links).


 Fig. 8. Overall network throughput vs.  $\mu$ , when  $K = 150$ .

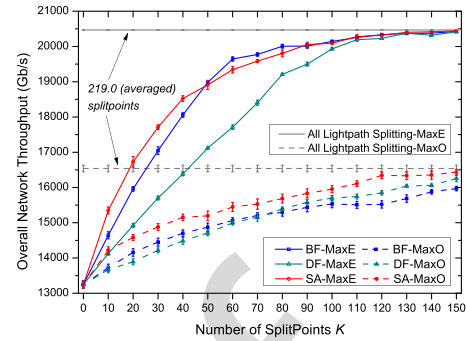
bandwidth between any node pair is randomly decided obeying a uniform distribution in the open interval (0, 75) Gb/s with 6.25 Gb/s granularity. For fairness among different simulation runs, the overall requested baseline bandwidth is fixed to be the average total bandwidth:  $\frac{0+75}{2} \cdot |N| \cdot (|N| - 1)$  Gb/s. Incremental index  $\mu$ , as defined before, controls the severity of traffic spikes.

In SA, initial temperature  $\tau_0 = 100 \cdot e^{K/10}$ , ending temperature  $\tau_e = 0.01/K^3$ , and cooling parameter  $\gamma = 0.95$ . The results shown are acquired from the average performance of 40 parallel simulations and results are plotted with confidence intervals at 95% confidence level.

### B. How Much Do We Gain?

Figs. 8-10 provide answers for how much throughput increase can we gain via different lightpath-splitting methods under different network settings. We see that MaxE policies always outperform MaxO policies, because they increase the capacity in different ways. MaxE maps the increased capacity in electrical layer, while MaxO puts the resource in optical layer. However, electrical-layer resources are more flexible to be used than optical-layer resources, which is enforced by spectrum continuity and contiguity constraints. We also find that, in most cases, SA policies outperform BF and DF policies, as expected, as SA can avoid local optima.

Fig. 8 presents relationship between overall network throughput (baseline and incremental traffic) and incremental index  $\mu$  when the number of SplitPoints (also the number of added transceiver pairs)  $K$  is 150. This figure presents a similar result as in Fig. 5(b) of network optimization results. We find that lightpath splitting policies can significantly increase network throughput with respect to *w/o lightpath splitting* whose throughput curve goes to flat at 15000 Gb/s. Besides, when incremental traffic is not so severe ( $\mu \in [0, 2]$ ), MaxE policies can provide as much throughput as the offered load (no traffic blocking). As  $\mu$  continues to be larger, MaxE policies (especially SA-MaxE) perform almost the same as


 Fig. 9. Overall network throughput vs.  $K$ , when  $\mu = 2$ .

*all lightpath splitting* (25000-30000 Gb/s, almost double the throughput of *w/o lightpath splitting*).

When we fix  $\mu$  to be 2, and observe how overall network throughput performs in different number of  $K$ , we get Fig. 9. For a given amount of incremental traffic, e.g.,  $\mu = 2$ , higher overall throughput can be gained as  $K$  becomes larger. It can be noticed that, when  $K$  grows to be 140 or 150, the throughput performance is almost the same as *all lightpath splitting*, whose  $K$  is around 219.0. This result reveals that a proper selection of SplitPoints is crucial for lightpath splitting.

For further understanding the relationships among throughput,  $K$ , and  $\mu$ , we plot Fig. 10, separating MaxE and MaxO results in two subfigures for readability. Here, we use normalized incremental throughput (with respect to the amount of incremental traffic) to fairly evaluate how much incremental traffic is served under different  $K$  and  $\mu$ . We find common trends, that in MaxE policies, BF performs better than DF. This is due to the fact that BF policies can involve more lightpaths into lightpath splitting without changing spectrum occupancy, resulting in more capacity on electrical layer. In MaxO policies, there is a crossing point that, when  $K$  is small, BF achieves better than DF, while DF gradually outperforms BF as the number of  $K$  increases. This is due to different lightpath spectrum reallocation results in BF and DF policies. In MaxO policies, splitting a lightpath harder (DF) may provide more available spectrum when the number of SplitLightpaths becomes larger as  $K$  increases.

### C. How Much Do We Compromise?

Fig. 11(a) presents the relationship between normalized affected traffic amount (with respect to the amount of traffic after Algorithm 1, when lightpath splitting is going to be triggered) vs.  $K$  when  $\mu = 2$ . For *all lightpath splitting* policies, there is around 54% traffic affected, the remaining 46% are those carried by one-hop lightpaths which cannot be split. We find that BF policies generally affect more traffic than SA and DF methods, while DF methods affect the least. This phenomenon is easy to understand because BF policies prefer to use as many lightpaths as possible, thus affecting more traffic, while DF policies tend to split lightpaths harder and involve the least number of lightpaths. For BF policies when  $K$  reaches 130 or larger, though they activate much less SplitPoints than *all lightpath splitting* (219.0 SplitPoints on average), the amount of affected traffic is the same. This discovery tells us that fewer SplitPoints does not necessarily mean less affected traffic. Once again it shows that a smart selection

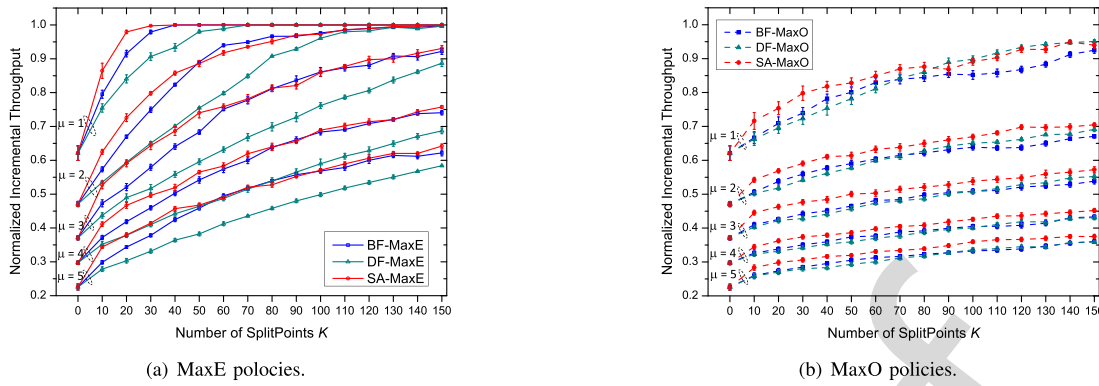


Fig. 10. Normalized incremental throughput (with respect to the amount of incremental traffic) vs. number of SplitPoints vs. incremental index  $\mu$ .

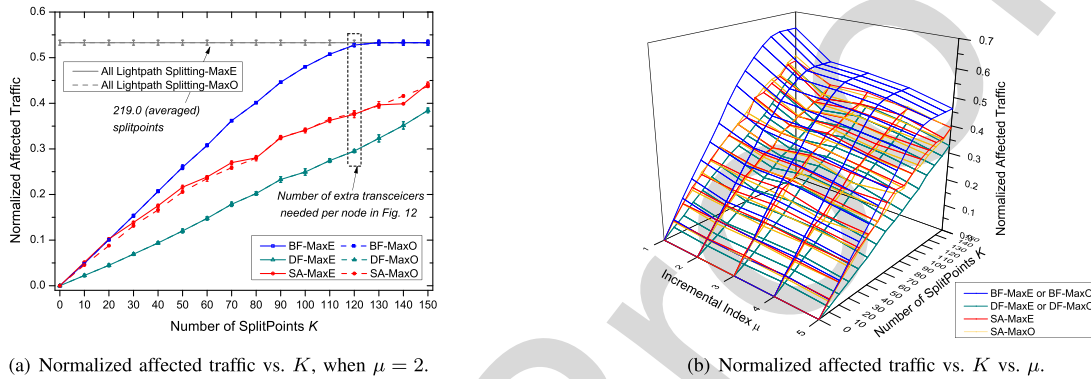


Fig. 11. Normalized affected traffic (with respect to the amount of supporting traffic after Algorithm 1).

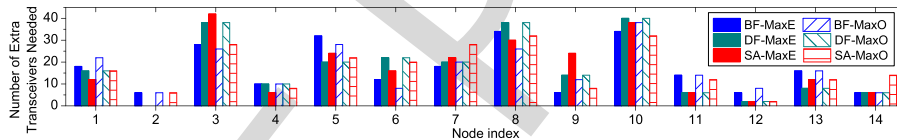


Fig. 12. The number of extra transceivers needed in each node, when  $\mu = 2$  and  $K = 120$ .

of SplitPoints is crucial from the perspective of affected traffic. Fig. 11(b) depicts the relationship among normalized affected traffic vs.  $K$  in different  $\mu$ . We find similar trends as in Fig. 11(a). Then, the conclusion drawn from Fig. 11(a) can be generalized to other situations with different  $\mu$ .

Fig. 12 shows how many extra transceivers are needed for each node of the network in a simulation run, when  $\mu = 2$  and  $K = 120$  (as discussed in Section III.E, the total number of increased transceivers is equal to twice the number of  $K$ ). We find that higher-degree nodes in the topology tend to need more additional transceivers during lightpath splitting.

In Fig. 13, we study how average traffic hops performs as  $K$  increases when  $\mu = 2$ . Here, we define average traffic hops per b/s to evaluate the average hops per unit bandwidth of all traffic on electrical layer. Multiple hops on electrical layer means multiple electrical processing, possibly resulting in higher end-to-end latency and energy consumption. We observe from Fig. 13 that MaxE policies result in larger traffic hops than MaxO, due to the fact that MaxO policies keep resources in the optical layer and leave more opportunities for setting up lightpaths to directly support traffic without intermediate nodes in electrical layer. Also, DF policies result in more traffic hops when  $K$  is larger (more than 40), and this is because DF policies tend to split lightpaths more aggressively.

Besides, the increased energy consumption is mainly caused by the increased number of transceivers, which is directly proportional to the number of  $K$  shown in almost all figures.

#### D. Trade-Off Curve by Pareto Front Analysis

As analyzed before, both logically in Section III and numerically in Section VI.B and VI.C, lightpath splitting can gain throughput increase with compromise of affecting existing traffic. What is the exact relationship between these two interacting user-experience-coupled variables? This answer is important for the network operator to choose a proper way to apply lightpath splitting.

In Fig. 14, we plot the Pareto front on throughput gained and traffic affected by lightpath splitting when  $\mu = 2$ . As expected, higher throughput is achieved at the cost of less unaffected traffic. A clear message from the figure is that *all lightpath splitting* is not an economical choice, as our proposed lightpath-splitting policies (both DF and SA for either MaxE or MaxO) can achieve similar throughput with much more unaffected traffic. We also learn from the figure that BF is not as efficient as DF and SA, because it always affects more traffic for a network throughput value. It is worth pointing out that, if we expect lightpath-splitting policies to return the highest throughput possible, BF policies are even worse than

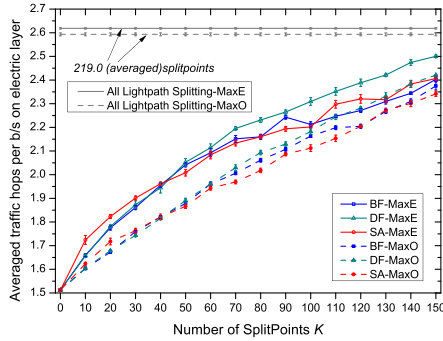


Fig. 13. Average traffic hops per b/s on electrical layer vs.  $K$ , when  $\mu = 2$ .

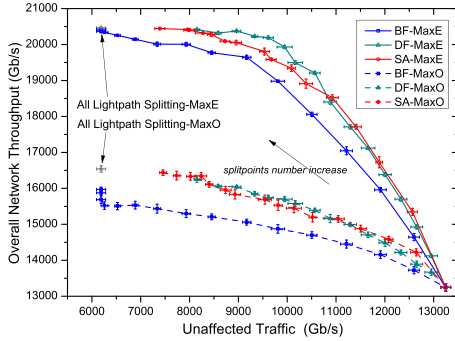


Fig. 14. Pareto front of throughput vs. unaffected traffic, when  $\mu = 2$ .

TABLE V  
ELAPSED RUNNING TIME (SECONDS) WHEN  $\mu = 2$

$K$	BF		DF		SA	
	MaxE	MaxO	MaxE	MaxO	MaxE	MaxO
10	1.096	1.229	1.209	1.240	337.390	374.280
80	0.176	0.940	0.355	0.956	137.635	545.693
150	0.109	0.823	0.117	0.808	63.593	611.494

all *lightpath splitting*, as BF policies achieve less throughput while affecting the same amount of traffic. There is a small upturned tail when the unaffected traffic is becoming small for BF policies. This is because BF policy has involved all lightpaths in lightpath splitting, and further lightpath splitting operations will be executed on those lightpaths that already have at least one SplitPoints.

Another observation that should be discussed is the slope of the Pareto-front curve. This slope can be regarded as the ratio of “gain” to “sacrifice”, describing the marginal utility of yield provided by lightpath splitting. When lightpath splitting is triggered, as  $K$  increases (from lower right to upper left on the figure), the slope is gradually diminishing to almost zero. This phenomenon teaches us that the first few SplitPoints with careful selection can gain more throughput increase than affected traffic; however, as the number of SplitPoints grows, the marginal utility of throughput increase diminishes. From the operators’ point of view, the incentive for introducing too many SplitPoints is weak. Therefore, a proper selection of the first few SplitPoints is critical. By using our proposed methods, the operator can address this problem proactively.

It should be highlighted that points on this Pareto-front curve represent the performance boundary for different lightpath-splitting policies. Moving along the curve by different points can provide the network operator various options to obtain throughput gains by affecting a fraction of

existing traffic using lightpath splitting. For different network topologies, spectrum resources, and traffic profiles, the exact location of the curve may vary with situations, but its trend of diminishing marginal throughput increase is general to other network instances.

### E. Execution Efficiency of the Proposed Algorithms

From Table V, we find that the execution time for greedy algorithms is on the order of several seconds, while SA-based algorithms take longer time (several minutes) because they need multiple iterations. Generally, the short-term traffic spikes studied in this paper last several hours or days, because they are caused by mega events as discussed in Section I. Therefore, the computational time of our proposed algorithms is acceptable to deal with short-term traffic spikes.

## VII. CONCLUSION

In this study, we proposed a novel network reconfiguration scheme with lightpath splitting to provision short-term traffic fluctuations. Lightpath splitting was first introduced to provide more elasticity for incremental traffic spikes. We mathematically formulated the lightpath splitting problem, and solved the optimization model in a small network example. We further devised scalable heuristic algorithms for lightpath splitting in practical networks. Simulation results showed that, by wisely selecting SplitPoints, we can achieve higher throughput gains for incremental traffic spikes with as little affected traffic as possible. A Pareto front for different lightpath-splitting policies was presented for the network operator to choose proper network configurations when facing traffic spikes.

### ACKNOWLEDGMENT

The authors would like to acknowledge P. J. Winzer, A. Cai, and Y. Li for enlightening discussions.

### REFERENCES

- [1] M. Gerla and L. Kleinrock, “On the topological design of distributed computer networks,” *IEEE Trans. Commun.*, vol. COMM-25, no. 1, pp. 48–60, Jan. 1977.
- [2] C.-Y. Hong *et al.*, “Achieving high utilization with software-driven WAN,” *ACM SIGCOMM Comput. Commun. Rev.*, vol. 43, no. 4, pp. 15–26, Aug. 2013.
- [3] G. Rizzelli, A. Morea, M. Tornatore, and O. Rival, “Energy efficient Traffic-Aware design of on-off multi-layer translucent optical networks,” *Comput. Netw.*, vol. 56, no. 10, pp. 2443–2455, Jul. 2012.
- [4] Y. Lui, G. Shen, and W. Shao, “Design for energy-efficient IP over WDM networks with joint lightpath bypass and router-card sleeping strategies,” *IEEE/OSA J. Opt. Commun. Netw.*, vol. 5, no. 11, pp. 1122–1138, Nov. 2013.
- [5] A. Morea, J. Perello, and S. Spadaro, “Traffic variation-aware networking for energy efficient optical communications,” in *Proc. ONDM*, Apr. 2013, pp. 29–34.
- [6] A. Morea, O. Rival, N. Brochier, and E. Le Rouzic, “Datarate adaptation for night-time energy savings in core networks,” *J. Lightw. Technol.*, vol. 31, no. 5, pp. 779–785, Mar. 1, 2013.
- [7] L. Stone. (2016). *Bringing Pokemon GO to Life on Google Cloud*, Google Cloud Platform Blog. <https://cloudplatform.googleblog.com/2016/09/bringing-Pokemon-GO-to-life-on-Google-Cloud.html>
- [8] Akamai. (2015). *Black Friday Traffic Spikes 109 Percent Over Average Pre-Holiday Activity*. [Online]. Available: <https://blogs.akamai.com/2015/12/2015-black-friday-traffic-spikes-109-percent-over-average-pre-holiday-activity.html>
- [9] J. Ryburn. (2017). *Black Friday vs. Cyber Monday: Traffic Insights from Kentik*. [Online]. Available: <https://www.kentik.com/black-friday-vs-cyber-monday-traffic-insights-from-kentik/>
- [10] (2016). *Boosting International Backbone Capacity for Global Events Such as the RIO 2016 Olympics* [Online]. Available: [http://us.ntt.net/news/viewFile.cfm/Capacity%20Magazine%20Aug%20Sept%202016%20NTT.pdf?file\\_id=200](http://us.ntt.net/news/viewFile.cfm/Capacity%20Magazine%20Aug%20Sept%202016%20NTT.pdf?file_id=200)

- [11] L. Chiaraviglio *et al.*, "Is green networking beneficial in terms of device lifetime?" *IEEE Commun. Mag.*, vol. 53, no. 5, pp. 232–240, May 2015.
- [12] L. Chiaraviglio *et al.*, "Lifetime-aware ISP networks: Optimal formulation and solutions," *IEEE/ACM Trans. Netw.*, vol. 25, no. 3, pp. 1924–1937, Jun. 2017.
- [13] J. Li, Z. Zhong, N. Hua, X. Zheng, and B. Zhou, "Balancing energy efficiency and device lifetime in TWDM-PON under traffic fluctuations," *IEEE Commun. Lett.*, vol. 21, no. 9, pp. 1981–1984, Sep. 2017.
- [14] A. P. Vela, M. Ruiz, and L. Velasco, "Distributing data analytics for efficient multiple traffic anomalies detection," *Comput. Commun.*, vol. 107, pp. 1–12, Jul. 2017.
- [15] L. Velasco *et al.*, "On-demand incremental capacity planning in optical transport networks," *IEEE/OSA J. Opt. Commun. Netw.*, vol. 8, no. 1, pp. 11–22, Jan. 2016.
- [16] L. Velasco, A. P. Vela, F. Morales, and M. Ruiz, "Designing, operating, and reoptimizing elastic optical networks," *J. Lightw. Technol.*, vol. 35, no. 3, pp. 513–526, Feb. 1, 2017.
- [17] D. Li, Y. Yu, J. Shi, and B. Zhang, "PALS: Saving network power with low overhead to ISPs and applications," *IEEE/ACM Trans. Netw.*, vol. 24, no. 5, pp. 2913–2925, Oct. 2016.
- [18] T. Hashiguchi, K. Tajima, Y. Takita, and T. Katagiri, "Techniques for agile network re-optimization following traffic fluctuations," in *Proc. OFC*, Mar. 2017, pp. 1–3.
- [19] E. Bouillet, J. F. Labourdette, R. Ramamurthy, and S. Chaudhuri, "Lightpath re-optimization in mesh optical networks," *IEEE/ACM Trans. Netw.*, vol. 13, no. 2, pp. 437–447, Apr. 2005.
- [20] F. Solano, "Analyzing two conflicting objectives of the WDM lightpath reconfiguration problem," in *Proc. IEEE GLOBECOM*, Nov./Dec. 2009, pp. 1–7.
- [21] F. Solano and M. Pióro, "Lightpath reconfiguration in WDM networks," *IEEE/OSA J. Opt. Commun. Netw.*, vol. 2, no. 12, pp. 1010–1021, Dec. 2010.
- [22] Z. Zhong *et al.*, "Energy efficiency and blocking reduction for tidal traffic via stateful grooming in IP-over-optical networks," *IEEE/OSA J. Opt. Commun. Netw.*, vol. 8, no. 3, pp. 175–189, Mar. 2016.
- [23] O. Gerstel, P. Lin, and G. Sasaki, "Wavelength assignment in a WDM ring to minimize cost of embedded SONET rings," in *Proc. IEEE INFOCOM*, Mar./Apr. 1998.
- [24] G. Mohan, P. H. H. Ernest, and V. Bharadwaj, "Virtual topology reconfiguration in IP/WDM optical ring networks," *Comput. Commun.*, vol. 26, no. 2, pp. 91–102, Feb. 2003.
- [25] N. Hua, H. Buchta, X. Zheng, H. Zhang, and B. Zhou, "Performance analysis of an improved postponed lightpath teardown strategy in multi-layer optical networks," in *Proc. ACP*, Nov. 2009, pp. 1–6.
- [26] A. Bocoi *et al.*, "Reach-dependent capacity in optical networks enabled by OFDM," in *Proc. OFC*, Mar. 2009, pp. 1–3.
- [27] T. Takagi *et al.*, "Dynamic routing and frequency slot assignment for elastic optical path networks that adopt distance adaptive modulation," in *Proc. OFC*, Mar. 2011, pp. 1–3.
- [28] T. Tanaka, T. Inui, A. Kadohata, W. Imajuku, and A. Hirano, "Multi-period IP-over-elastic network reconfiguration with adaptive bandwidth resizing and modulation," *IEEE/OSA J. Opt. Commun. Netw.*, vol. 8, no. 7, pp. A180–A190, Jul. 2016.
- [29] G. Huang, Y. Miyoshi, A. Maruta, Y. Yoshida, and K. Kitayama, "All-optical OOK to 16-QAM modulation format conversion employing nonlinear optical loop mirror," *J. Lightw. Technol.*, vol. 30, no. 9, pp. 1342–1350, May 1, 2012.
- [30] R. Singh, M. Ghobadi, K. T. Foerster, M. Filer, and P. Gill, "Run, walk, crawl: Towards dynamic link capacities," in *Proc. ACM Workshop Hot Topics Netw.*, Nov. 2017, pp. 143–149.
- [31] R. Singh, M. Ghobadi, K. T. Foerster, M. Filer, and P. Gill, "RADWAN: Rate adaptive wide area network," in *Proc. SIGCOMM*, Aug. 2018, pp. 547–560.
- [32] S. S. Savas, M. F. Habib, M. Tornatore, F. Dikbiyik, and B. Mukherjee, "Network adaptability to disaster disruptions by exploiting degraded-service tolerance," *IEEE Commun. Mag.*, vol. 52, no. 12, pp. 58–65, Dec. 2014.
- [33] C. S. K. Vadrevu, R. Wang, M. Tornatore, C. U. Martel, and B. Mukherjee, "Degraded service provisioning in mixed-line-rate WDM backbone networks using multipath routing," *IEEE/ACM Trans. Netw.*, vol. 22, no. 3, pp. 840–849, Jun. 2014.
- [34] W. Hou, Y. Zong, X. Zhang, and L. Guo, "Adaptive service degradation in converged optical and data center networks," in *Proc. ACP*, Nov. 2014, pp. 1–3.
- [35] M. Wang, M. Furdek, P. Monti, and L. Wosinska, "Restoration with service degradation and relocation in optical cloud networks," in *Proc. ACP*, Nov. 2015, p. 3, Paper ASuSF-2.
- [36] R. B. R. Lourenço, M. Tornatore, C. U. Martel, and B. Mukherjee, "Running the network harder: Connection provisioning under resource crunch," *IEEE Trans. Netw. Service Manage.*, vol. 15, no. 4, pp. 1615–1629, Dec. 2018.
- [37] Z. Zhong *et al.*, "On QoS-assured degraded provisioning in service-differentiated multi-layer elastic optical networks," in *Proc. IEEE GLOBECOM*, Dec. 2016, pp. 1–5.
- [38] K. Christodoulopoulos, I. Tomkos, and E. A. Varvarigos, "Elastic bandwidth allocation in flexible OFDM-based optical networks," *J. Lightw. Technol.*, vol. 29, no. 9, pp. 1354–1366, May 1, 2011.
- [39] J. Zhao, S. Subramaniam, and M. Brandt-Pearce, "Virtual topology mapping in elastic optical networks," in *Proc. IEEE ICC*, 2013, pp. 3904–3908.
- [40] P. Chimento and J. Ishac, *Defining Network Capacity*, document IETF RFC 5136, 2008.
- [41] Y. Li and D. C. Kilper, "Optical physical layer SDN," *IEEE/OSA J. Opt. Commun. Netw.*, vol. 10, no. 1, pp. A110–A121, Jan. 2018.
- [42] D. C. Kilper, C. A. White, and S. Chandrasekhar, "Control of channel power instabilities in constant-gain amplified transparent networks using scalable mesh scheduling," *J. Lightw. Technol.*, vol. 26, no. 1, pp. 108–113, Jan. 1, 2008.
- [43] F. Smyth, D. C. Kilper, S. Chandrasekhar, and L. P. Barry, "Applied constant gain amplification in circulating loop experiments," *J. Lightw. Technol.*, vol. 27, no. 21, pp. 4686–4696, 2009.
- [44] D. C. Kilper, M. Bhopalwala, H. Rastegarfar, and W. Mo, "Optical power dynamics in wavelength layer software defined networking," in *Proc. Photonic Netw. Devices*, Jan. 2015, p. 3, Paper NeT2F.2.
- [45] P. J. Lin, "Reducing optical power variation in amplified optical network," in *Proc. Int. Conf. Commun. Technol.*, Apr. 2003, pp. 42–47.
- [46] D. A. Mongardien, S. Borne, C. Martinelli, C. Simonneau, and D. Bayart, "Managing channels add/drop in flexible networks based on hybrid Raman/erbium amplified spans," *Âzin Proc. ECOC*, Sep. 2006, pp. 1–2.
- [47] A. S. Ahsan *et al.*, "Excursion-free dynamic wavelength switching in amplified optical networks," *IEEE/OSA J. Opt. Commun. Netw.*, vol. 7, no. 9, pp. 898–905, Sep. 2015.
- [48] Y. Huang, P. B. Cho, P. Samadi, and K. Bergman, "Power excursion mitigation for flexgrid defragmentation with machine learning," *IEEE/OSA J. Opt. Commun. Netw.*, vol. 10, no. 1, pp. A69–A76, Jan. 2018.
- [49] W. Mo *et al.*, "Deep-neural-network-based wavelength selection and switching in ROADM systems," *IEEE/OSA J. Opt. Commun. Netw.*, vol. 10, no. 10, pp. D1–D11, Oct. 2018.
- [50] R. Luo, N. Hua, X. Zheng, and B. Zhou, "Fast parallel lightpath re-optimization for space-division multiplexing optical networks based on time synchronization," *IEEE/OSA J. Opt. Commun. Netw.*, vol. 10, no. 1, pp. A8–A19, 2018.
- [51] X. Jin *et al.*, "Dynamic scheduling of network updates," *ACM SIGCOMM Comput. Commun. Rev.*, vol. 44, no. 4, pp. 539–550, Aug. 2014.
- [52] Z. Zhu, W. Lu, L. Zhang, and N. Ansari, "Dynamic service provisioning in elastic optical networks with hybrid single-/multi-path routing," *J. Lightw. Technol.*, vol. 31, pp. 15–22, Jan. 1, 2013.
- [53] G. Charlet *et al.*, "Transmission of 81 channels at 40Gbit/s over a transpacific-distance erbium-only link, using PDM-BPSK modulation, coherent detection, and a new large effective area fibre," in *Proc. ECOC*, Sep. 2008, pp. 1–2.
- [54] M. Salsi *et al.*, "WDM 200 Gb/s single-carrier PDM-QPSK transmission over 12,000 km," in *Proc. ECOC*, Sep. 2011, pp. 1–3.
- [55] M. Salsi *et al.*, "31 Tb/s transmission over 7, 200 km using 46 Gbaud PDM-8QAM with optimized error correcting code rate," in *Proc. OECC*, Jun./Jul. 2013, pp. 1–2.
- [56] W. Idler, F. Buchali, and K. Schuh, "Experimental study of symbol-rates and MQAM formats for single carrier 400 Gb/s and few carrier 1 Tb/s options," in *Proc. OFC*, Mar. 2016, pp. 1–3.
- [57] P. J. Winzer, "High-spectral-efficiency optical modulation formats," *J. Lightw. Technol.*, vol. 30, no. 24, pp. 3824–3835, Dec. 2012.
- [58] Y. Wang, X. Cao, and Y. Pan, "A study of the routing and spectrum allocation in spectrum-sliced elastic optical path networks," in *Proc. IEEE INFOCOM*, Apr. 2011, pp. 1503–1511.
- [59] H. Zhu, H. Zang, K. Zhu, and B. Mukherjee, "A novel generic graph model for traffic grooming in heterogeneous WDM mesh networks," *IEEE/ACM Trans. Netw.*, vol. 11, no. 2, pp. 285–299, Apr. 2003.
- [60] M. Jinno *et al.*, "Distance-adaptive spectrum resource allocation in spectrum-sliced elastic optical path network," *IEEE Commun. Mag.*, vol. 48, no. 8, pp. 138–145, Aug. 2010.
- [61] B. Mukherjee, D. Banerjee, S. Ramamurthy, and A. Mukherjee, "Some principles for designing a wide-area WDM optical network," *IEEE/ACM Trans. Netw.*, vol. 4, no. 5, pp. 684–696, Oct. 1996.
- [62] K. Zhu and B. Mukherjee, "Traffic grooming in an optical WDM mesh network," *IEEE J. Sel. Areas Commun.*, vol. 20, no. 1, pp. 122–133, Jan. 2002.
- [63] S. Zhang, C. Martel, and B. Mukherjee, "Dynamic traffic grooming in elastic optical networks," *IEEE J. Sel. Areas Commun.*, vol. 31, no. 1, pp. 4–12, Jan. 2013.
- [64] J.-F. P. Labourdette and A. S. Acampora, "Logically rearrangeable multihop lightwave networks," *IEEE Trans. Commun.*, vol. 39, no. 8, pp. 1223–1230, Aug. 1991.